Serber symmetry, large N_c, and Yukawa-like one-boson exchange potentials

A. Calle Cordón* and E. Ruiz Arriola†

Departamento de Física Atómica, Molecular y Nuclear, Universidad de Granada, E-18071 Granada, Spain

(Received 17 April 2009; published 29 July 2009)

The Serber force has relative orbital parity symmetry and requires vanishing NN interactions in partial waves with odd angular momentum. We illustrate how this property is well fulfilled for spin triplet states with odd angular momentum and violated for odd singlet states for realistic potentials but fails for chiral potentials. The analysis is carried out in terms of partial wave sum rules for NN phase shifts, r-space potentials at long distances, and $V_{\text{low }k}$ potentials. We analyze how Serber symmetry can be accommodated within a large-N_c perspective when interpreted as a long-distance symmetry. A prerequisite for this is the numerical similarity of the scalar and vector meson resonance masses. The conditions under which the resonance exchange potential can be approximated by a Yukawa form are also discussed. Although these masses arise as poles on the second Riemann in $\pi\pi$ scattering, we find that within the large-N_c expansion the corresponding Yukawa masses correspond instead to a well-defined large-N_c approximation to the pole that cannot be distinguished from their location as Breit-Wigner resonances.

DOI: 10.1103/PhysRevC.80.014002 PACS number(s): 13.75.Cs, 03.65.Nk, 11.10.Gh, 21.30.Fe

I. INTRODUCTION

The modern theory of nuclear forces [1] aims at a systematic and model-independent derivation of the forces between nucleons in harmony with the symmetries of quantum chromodynamics. Actually, an outstanding feature of nuclear forces is their exchange character. Many years ago, Serber postulated an interesting symmetry for the nucleon-nucleon system based on the observation that at low energies the proton-proton and neutron-proton differential cross section are symmetric functions in the center-of-mass (CM) scattering angle around 90°. This orbital parity symmetry corresponds to the transformation $\theta \to \pi - \theta$ in the scattering amplitude and was naturally explained by assuming that the potential was vanishing for partial waves with odd angular momentum. Such a Serber force is a 50/50 mixture of ordinary and space exchange forces.[1] Specific attempts were directed toward the verification of such a property [4]. (See Refs. [6] and [7] for early and comprehensive reviews.) This symmetry was shown to hold for the NN system, up to relatively high energies [8]. However, such a force was also found to be incompatible with the requirement of nuclear matter saturation [9] as well as with the underlying meson forces mediated by one- and two-pion exchange [10]. These puzzling inconsistencies were cleared up when it was understood that only singular Serber forces could provide saturation [11]. Old phase-shift analyses [12] confirm the rough Serber exchange character of nuclear forces. Many theories of nuclear structure [13], nuclear matter [14], and nuclear reactions [15–17] use Serber forces both for their simplicity as well as their phenomenological success in the low- and medium-energy region. The possibility of implementing Serber forces in the nuclear potential was envisaged in Skyrme's seminal paper [18]. Modern versions (SLy4) of the Skyrme effective interactions [19] implement the symmetry explicitly. In a recent paper [20] a novel fitting strategy has been proposed for the coupling constants of the nuclear energy density functional, which focus on single-particle energies rather than ground-state bulk properties, yielding naturally an almost perfect fulfillment of Serber symmetry.

A vivid demonstration of the Serber symmetry is shown in Fig. 1, where the np differential cross section is plotted for several CM momenta using the partial wave analysis (PWA) and the high quality potentials [21,22] carried out by the Nijmegen group. Although discrepancies regarding the comparison between forward and backward directions show that this symmetry breaks down at short distances, the intermediate-energy region does exhibit Serber symmetry. In any case it is interesting to see that even though intermediate-energy region departures from the symmetry can be seen, the symmetry point is shifted a few degrees toward values lower than 90° for increasing energies. Although these are well-established features of the NN interaction, it is amazing that such a time-honored force and gross feature of the NN interaction, even if it does not hold in the entire range, has no obvious explanation from the more fundamental and QCD motivated side. To our knowledge this topic has not been explicitly treated in any detail in the literature and no attempts have been made to justify this evident but, so far, accidental symmetry. The present paper tries to fill this gap by unveiling Serber symmetry at the relevant scales from current theoretical approaches to the NN problem, looking for its consequences in nuclear physics and analyzing its possible origin. Of course, a definite explanation might finally be given by lattice QCD calculations, for which incipient results exist already in the case of S-wave interactions [23,24].

*alvarocalle@ugr.es

†earriola@ugr.es

[1] Apparently there is no reference for Serber's work (see, e.g., Ref. [2]). Serber suggests that the term "Serber force" was coined by E. Wigner [3]. The first known documented quotation we could find appears in Ref. [4]. The first 1947 edition of Ref. [5] does not contain this term but the second 1956 edition does. We thank R. Machleidt for pointing out this fact.

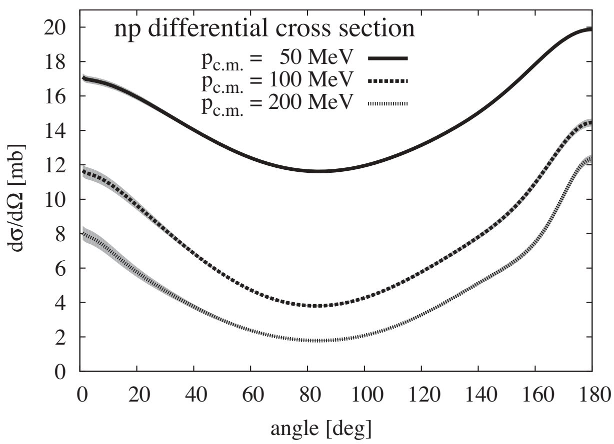

FIG. 1. Differential cross section for *np* scattering at several CM momenta (in MeV). The error band reflects the partial wave analysis (PWA) and high-quality potentials of the Nijmegen group [21,22]. Serber symmetry implies that the functions should be symmetric in the CM scattering angle around 90°.

The motivation for the present study arises from our recent analysis [25] of an equally old symmetry, the SU(4)-spin-isospin symmetry proposed independently by Wigner and Hund [26,27] by introducing the concept of *long-distance symmetry*. Specifically, we showed how a symmetry of the potential at any nonvanishing but arbitrarily small distance does not necessarily imply a symmetry of the S matrix that may be directly observed at all energies.[2] This provided an interpretation of the role played by the Wigner symmetry in the S waves; the potentials for the two-nucleon $^1S_0$ and $^3S_1$ states are *identical* whereas the corresponding phase shifts are very different at all measurable energies. Furthermore, we showed how a sum rule for SU(4) supermultiplet phase shifts splitting from spin-orbit and tensor interactions is well fulfilled for noncentral L-even waves and strongly violated in L-odd waves, where a Serber-like symmetry holds instead. In Sec. II we review the sum rules obtained from our previous work for the partial wave phase shifts and show how their potential counterpart is also well verified by high-quality NN potentials (i.e., potentials that have $\chi^2/\mathrm{DOF} \sim 1$). Obviously, *any* NN potential explaining the data will necessarily comply to odd-L Serber symmetry as a whole; a less trivial matter is to check whether this is displayed *explicitly* by the potential and to determine the relevant ranges where the symmetry is located. At long distances the interaction is given by one-pion exchange (OPE), which is Wigner symmetric for even-L waves and provides a $1/9$ violation of Serber symmetry for odd-L waves at long distances. Phenomenological potentials seem to provide different ranges for each symmetry. In Sec. III we analyze the signatures of the symmetry and its range from several viewpoints including the PWA of the Nijmegen group, the $V_{\mathrm{low}\,k}$ approach, and chiral two-pion exchange. In Sec. IV we digress on the meaning of counterterms as a diagnostics tool to characterize a long-distance symmetry from both perturbative as well as Wilsonian renormalization points of view, the implications for Skyrme forces, and the resonance saturation of chiral forces.

The evidence for both even-L Wigner and odd-L Serber symmetries is so overwhelming that we feel a pressing need for an explanation more closely based on our current knowledge of strong interactions and QCD. Actually, central to our analysis will be the use of the large-N_c expansion [28,29] (for comprehensive reviews see, e.g., Refs. [30–32]). Here N_c is the number of colors and in this limit the strong coupling constant scales as $\alpha_s \sim 1/N_c$. For color singlet states the picture is that of infinitely many stable mesons and glueballs, whose masses behave as $m \sim N_c^0$ and widths as $\Gamma \sim 1/N_c$, and heavy baryons, whose masses scale as $M \sim N_c$. This limit also fixes the interactions among hadrons. Meson-meson interactions are weak since they scale as $1/N_c$, meson-baryon interactions scale as $\sim N_c^0$ and baryon-baryon interactions are strong as they scale as $\sim N_c$. Although the pattern of SU(4)-symmetry breaking complies to the large-N_c expectations [33,34], a somewhat unexpected conclusion, we also pointed out that Serber symmetry, while not excluded for odd-L waves, *was not* a necessary consequence of large N_c. The search for an explanation of the Serber force requires more detailed information than in the case of Wigner symmetry. In any case, our interpretation of Wigner symmetry as a long-distance symmetry suggests that at best we can only interpret this large-N_c prediction not literally but in a more restrictive sense (i.e., as a feature of potentials and *not* of the S matrix).

In Sec. V we approach Serber symmetry from a large-N_c perspective and make explicit use of the fact that the meson exchange picture seems justified [35]. Actually, within such a realization a necessary prerequisite for the validity of the symmetry would be a numerical similarity of the scalar and vector meson masses. This poses a puzzle since, as is well known, these mesons arise as resonances in $\pi\pi$ scattering as poles in the second Riemann sheet, yielding the values $\sqrt{s_\sigma} = m_\sigma - i\Gamma_\sigma/2 = 441^{+16}_{-8} - i272^{+9}_{-12}$ MeV [36] and $\sqrt{s_\rho} = m_\rho - i\Gamma_\rho/2 = 775.49 \pm 0.34 - i149.4 \pm 1.0$ MeV [37]. The scalar and vector masses and widths are sufficiently different as to make one question whether one is close to the Serber limit. In Sec. VI we review the role of two-pion exchange and analyze the resonances as well as the generation of Yukawa potentials from the exchange of $\pi\pi$ resonances from a large-N_c viewpoint. An important result of the present paper is to show that the Yukawa masses are determined as large-N_c approximations to the pole position, which cannot be distinguished from the Breit-Wigner resonance. In light of this result it is possible indeed from the large-N_c side to envisage a rationale for the Serber symmetry. Finally, in Sec. VII we present our conclusions and summarize our main points.

II. LONG-DISTANCE SYMMETRY AND WEIGHTED AVERAGE POTENTIALS

When discussing and analyzing symmetries in nuclear physics quantitatively we find it convenient to delineate the

[2] In renormalization language this corresponds to a symmetry of the potential for any nonvanishing distance that is not shared by the counterterms.

scale where they supposedly operate. As we see from Fig. 1, Serber symmetry does not work all over the range nor equally well for all energies. Thus, we expect to see the symmetry in the medium- and long-distance region, precisely where a reliable theoretical description in terms of potentials becomes possible. Although this is easily understood, it is less trivial to implement these features in a model-independent formulation. Furthermore, as we see from Fig. 1 there are some small deviations and it may be advisable to find out not only the origin of the symmetry but also the sources of this symmetry breaking.

For the purpose of the present discussion we will separate the NN potential as the sum of central components and noncentral ones, which will be assumed to be small,

$$\mathcal{V}_{NN} = V_0 + V_1, \tag{1}$$

where $[\vec{L}, V_0] = 0$ whereas $[\vec{J}, V_1] = 0$ and $[\vec{L}, V_1] \neq 0$. Specifically, for the central part we take

$$V_0 = V_C + \tau W_C + \sigma V_S + \tau\sigma W_S, \tag{2}$$

and the noncentral part is

$$V_1 = (V_T + \tau W_T)S_{12} + (V_{LS} + \tau W_{LS})L \cdot S. \tag{3}$$

Here $\tau = \tau_1 \cdot \tau_2$ and $\sigma = \sigma_1 \cdot \sigma_2$, with σ_i and τ_i the Pauli matrices representing the spin and isospin, respectively, of the nucleon i. The tensor operator is $S_{12} = 3\sigma_1 \cdot \hat{x}\sigma_2 \cdot \hat{x} - \sigma_1 \cdot \sigma_2$ and $L \cdot S$ corresponds to the spin-orbit term. The total potential commutes with the total angular momentum $J = L + S$. However, we will start by assuming that the potential is central and that the breaking in orbital angular momentum is small.

We proceed in first-order perturbation theory, by using the central symmetric distorted waves as the unperturbed states. Note that $\tau = \tau_1 \cdot \tau_2 = 2T(T+1) - 3$ and $\sigma = \sigma_1 \cdot \sigma_2 = 2S(S+1) - 3$ and the Pauli principle requires $(-)^{S+T+L} = -1$. The corresponding zeroth-order wave function is of the form

$$\Psi(\vec{x}) = \frac{u_L^{ST}(r)}{r} Y_{LM_L}(\hat{x}) \chi^{SM_S} \phi^{TM_T}, \tag{4}$$

with χ^{SM_S} and ϕ^{TM_T} spinors and isospinors with good total spin $S = 0, 1$ and isospin $T = 0, 1$, respectively. The radial wave functions satisfy the asymptotic boundary conditions

$$u_L^{ST}(r) \to \sin\left(kr - \frac{L\pi}{2} + \delta_L^{ST}\right), \tag{5}$$

where k is the CM momentum. From the central potential assumption it is clear that partial waves do not depend on the total angular momentum and so we would have, for example, $\delta_{^3P_0} = \delta_{^3P_1} = \delta_{^3P_2}$ and so on, in complete contradiction to the data. As is well known the spin-orbit interaction lifts the independence on the total angular momentum, via the operator $\vec{L} \cdot \vec{S}$. Moreover, the tensor coupling operator, S_{12}, mixes states with different orbital angular momentum, so to account for the J dependence we proceed in first-order perturbation theory in the spin-orbit and tensor potentials using the orbital symmetric distorted waves as the unperturbed states. Note that this is *not* the standard Born approximation where all components of the potential are treated perturbatively. According to a previous calculation (see Appendix D of Ref. [25]) the correction to the phase shift to first order reads

$$\Delta\delta_{JL}^{ST} = -\frac{M}{p}\int_0^\infty dr\, u_L^{ST}(r)^\dagger \Delta V u_L^{ST}(r), \tag{6}$$

so that the perturbed eigenphases become

$$\delta_{JL}^{ST} = \delta_L^{ST} + \Delta\delta_{JL}^{ST}. \tag{7}$$

Note that to this order the mixing phases vanish, $\Delta\epsilon_J = 0$, and there is no difference between the eigen phase shifts or the nuclear bar phase shifts. Note that although the spin-orbit operator $\vec{L} \cdot \vec{S}$ lifts the independence on the total angular momentum and the tensor coupling operator, S_{12}, mixes states with different orbital angular momentum, these two perturbations leave the center of the orbital multiplets unchanged. Actually, since

$$\sum_{J=L-1}^{L+1} (2J+1)\left(\Delta V_J^{10}\right)_{L,L} = 0, \tag{8}$$

one has

$$\sum_{J=L-1}^{L+1} (2J+1)\Delta\delta_{LJ}^{10} = 0. \tag{9}$$

As a consequence

$$\bar{\delta}_L^{ST} = \frac{\sum_{J=L-1}^{L+1}(2J+1)\delta_{LJ}^{ST}}{(2L+1)3} = \delta_L^{ST}. \tag{10}$$

Thus, to first order we may define a common *mean* phase obtained as the one obtained from a *mean* potential

$$\bar{V}_{^3L}(r) = \frac{\sum_{J=L-1}^{L+1}(2J+1)V_{^3L_J}(r)}{3(2L+1)}. \tag{11}$$

It is in terms of these potentials where we expect to formulate the verification of a given symmetry. This is nothing but the standard procedure of verifying a symmetry between multiplets by defining first the center of the multiplet.[3] Now, Serber symmetry requires

$$V_{^1L}(r) = V_{^3L}(r) = 0, \quad \text{odd } L, \tag{12}$$

whereas Wigner symmetry requires

$$V_{^3L}(r) = V_{^1L}(r), \quad \text{all } L. \tag{13}$$

Clearly these two requirements are incompatible except when all potentials vanish. In Fig. 2 we plot the Argonne V-18 potentials [38] for the center of the orbital multiplets. Thus

[3]A familiar example is provided by the verification of SU(3) in the baryon spectrum. Although the symmetry is rough the Gell-Mann-Okubo formula works rather well after it has been broken by a symmetry-breaking term.

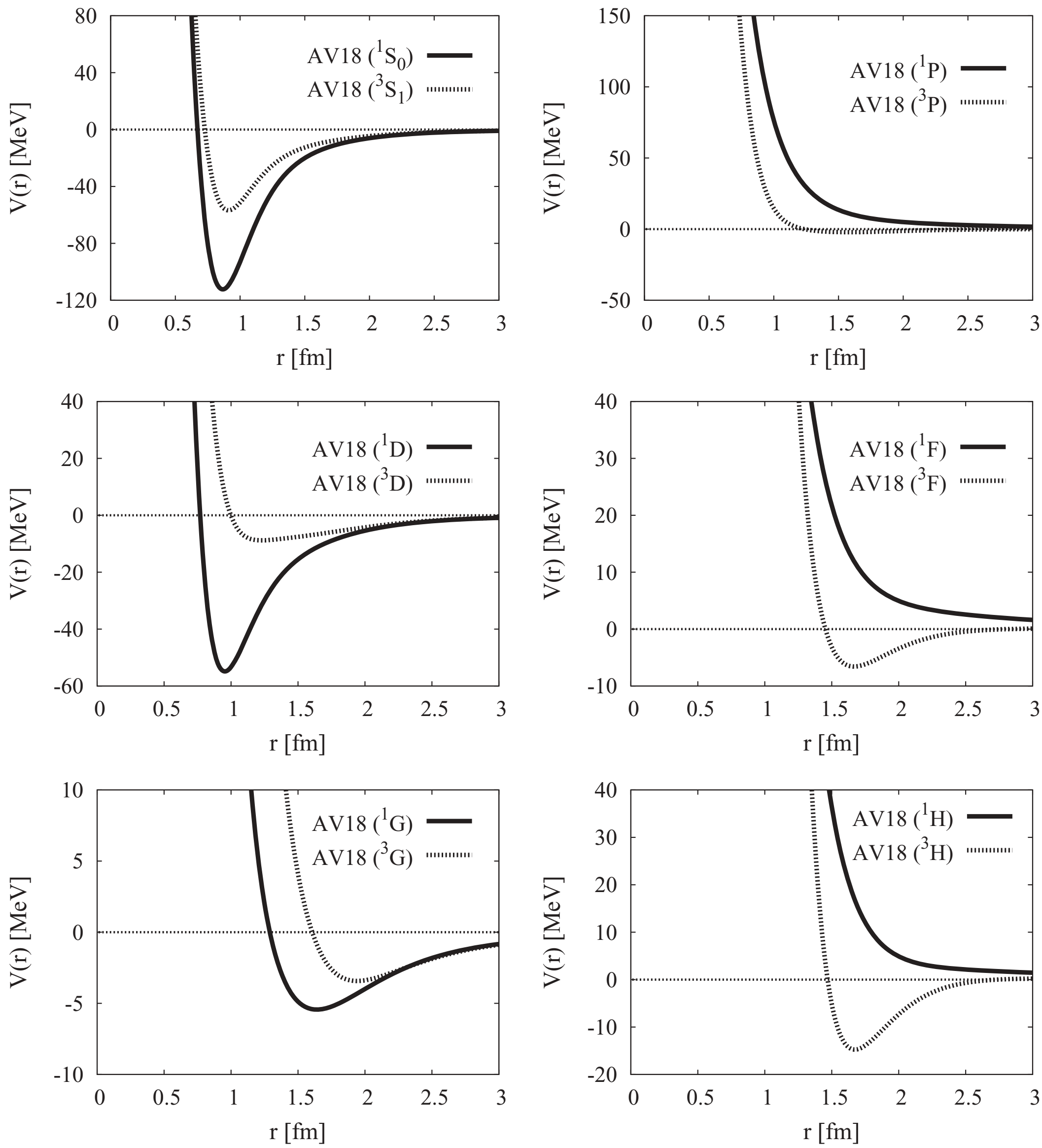

FIG. 2. Argonne V-18 potentials [38] for the center of the Serber-Wigner multiplets. Wigner symmetry requires singlet and triplet potentials to coincide. Serber symmetry implies vanishing odd-L partial waves. Even-L waves possess Wigner symmetry whereas odd-L triplet waves exhibit Serber symmetry.

the potentials suggest instead that for $r > 1.5$ fm

$$V_{^3L}(r) \ll V_{^1L}(r), \qquad \text{odd } L, \tag{14}$$

$$V_{^3L}(r) \sim V_{^1L}(r), \qquad \text{even } L; \tag{15}$$

that is, Wigner symmetry is fulfilled for *even-L* states whereas Serber symmetry holds for odd-L *triplet* states at distances above 1.5 fm, in agreement with the expectations spelled out at the beginning of this section. The parallel statements for phase shifts have been developed in detail in Ref. [25] (see Fig. 3), where the relation of long-distance symmetry and renormalization has been stressed. The remarkable aspect, already discussed there, is that the symmetry pattern, although incompatible with Wigner symmetry for odd-L states, is fully compatible with large-N_c expectations [34]. It does not explain, however, *why* Serber symmetry is a good one.

III. SEARCHING THE SYMMETRY

Most modern potential models of the NN interaction include OPE as the dominant longest range contribution. However, they differ at short distances where many effects compete and even are written in quite different forms (energy dependent, momentum dependent, angular momentum dependent, etc.). These ambiguities are of course compatible with the inverse scattering problem and manifest mainly in the off-shell behavior of the NN forces. The relevant issue within the present context regards the *range* and *form* of current NN interactions from the view point of long-distance symmetries. Any potential fitting to the elastic scattering data must possess the symmetries displayed by the phase-shift sum rules as we see in Fig. 3. However, it is not obvious that potentials display the symmetry explicitly.

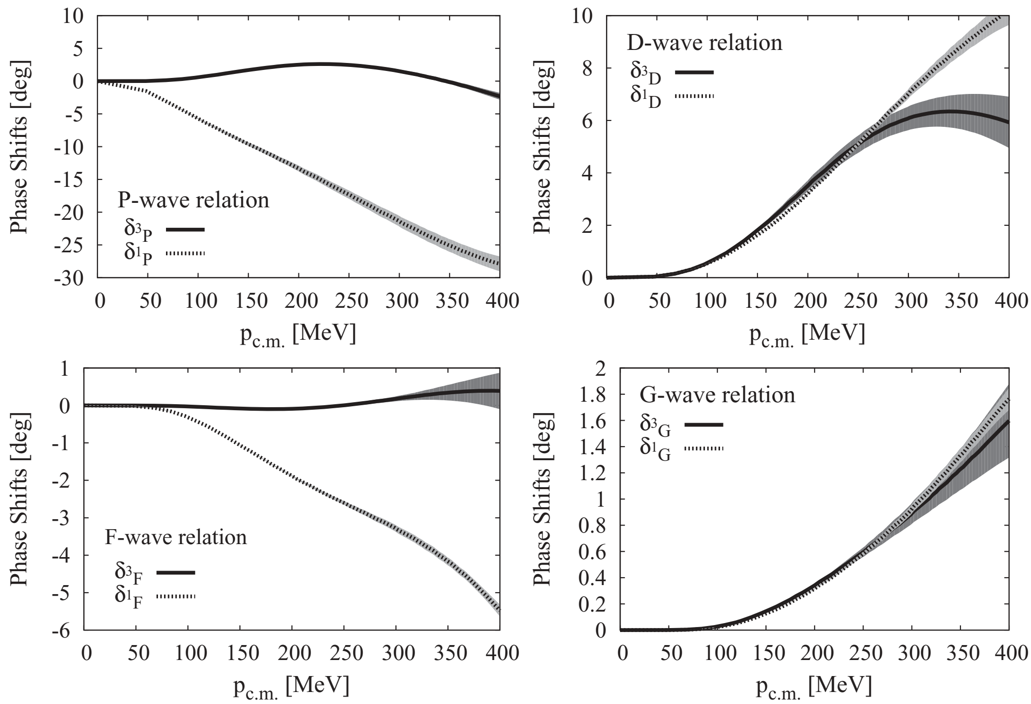

FIG. 3. Average values of the phase shifts [21] (in degrees) as a function of the CM momentum (in MeV). (Upper left panel) P waves. (Upper right panel) D waves. (Lower left panel) F waves. (Lower right panel) G waves. According to the Wigner symmetry $\delta_{^1L} = \delta_{^3L}$. Serber symmetry implies $\delta_{^3L} = 0$ for odd L. One sees that L-even waves satisfy Wigner symmetry whereas L-odd spin triplet waves satisfy Serber symmetry.

A. One-pion exchange

The OPE potential reads

$$V^\pi(r) = \tau\left[\sigma W_S^\pi(r) + S_{12} W_T^\pi(r)\right]. \tag{16}$$

Although OPE complies to the Wigner symmetry it does not embody exactly the Serber symmetry. Actually, we get for even-L waves

$$V^\pi_{^1S}(r) = V^\pi_{^1D}(r) = V^\pi_{^1G}(r) = -3W_S^\pi(r), \tag{17}$$
$$V^\pi_{^3S}(r) = V^\pi_{^3D}(r) = V^\pi_{^3G}(r) = -3W_S^\pi(r), \tag{18}$$

and for odd-L waves we have

$$V^\pi_{^1P}(r) = V^\pi_{^1F}(r) = V^\pi_{^1H}(r) = 9W_S^\pi(r), \tag{19}$$
$$V^\pi_{^3P}(r) = V^\pi_{^3F}(r) = V^\pi_{^3H}(r) = W_S^\pi(r). \tag{20}$$

The factor 9 for the singlet to triplet ratio is nonetheless a close approximation to the Serber limit in a region where the potential is anyhow small. These OPE relations are verified in practice for distances above 3–4 fm. As we see from Fig. 2 the vanishing of the ^3P potential happens down to the region around 1.5 fm. For smaller distances, potential models start deviating from each other (see, e.g., Ref. [22]) but this vanishing of the ^3P potential is a common feature that occurs *beyond* the validity of OPE.

B. Boundary conditions (alias $V_{\text{high } R}$)

We now analyze the symmetry issue for the highly successful PWA [21] of the Nijmegen group. There, a OPE potential is used down to $r_c = 1.4$ fm and the interaction below that distance is represented by a boundary condition determined by a square-well potential with an energy-dependent height,

$$2\mu V_{S,\beta}(k^2) = \sum_{n=0}^{N} a_{n,\beta} k^{2n}, \tag{21}$$

where β stands for the corresponding channel, so that the total potential reads

$$V_\beta(r) = \left[V_\beta^\pi(r) + V_\beta^{\text{int}}(r)\right]\theta(r - r_c) + V_{S,\beta}(k^2)\theta(r_c - r), \tag{22}$$

where $V_\beta^{\text{int}}(r)$ is a phenomenological intermediate-range potential that acts in the region $1.4 \leqslant r \leqslant 2.0$ fm. Then, for the center of the L multiplets (with V in MeV and k in fm) we have

$$V_{S,^1P}(k^2) = 139.438 - 23.412k^2 + 2.479k^4, \tag{23}$$
$$V_{S,^3P}(k^2) = 14.666 + 0.92k^2 + 0.029k^4, \tag{24}$$
$$V_{S,^1F}(k^2) = 248.73, \tag{25}$$
$$V_{S,^3F}(k^2) = -33.08 + 5.90k^2, \tag{26}$$

where, again, we see that Serber symmetry takes place since $V_{S,^3P}(k^2) \ll V_{S,^1P}(k^2)$ and $V_{S,^3F}(k^2) \ll V_{S,^1F}(k^2)$. Actually, the factor is strikingly similar to the 1/9 of the OPE interaction, which in the analysis holds up to $r_c = 1.4$ fm. Thus, in the Nijmegen PWA decomposition of the interaction we find the remarkable relation

$$V_{^3L}(r) \ll V_{^1L}(r), \quad \text{odd } L, \quad \text{all } r, \tag{27}$$

showing that there is Serber symmetry in the short-range piece of the potential. However, the even partial waves yield

$$V_{S,{}^1S}(k^2) = -17.813 - 1.016k^2 + 2.564k^4, \quad (28)$$

$$V_{S,{}^3S}(k^2) = -40.955 + 4.714k^2 + 1.779k^4, \quad (29)$$

$$V_{S,{}^1D}(k^2) = 61.42 - 15.678k^2, \quad (30)$$

$$V_{S,{}^3D}(k^2) = 28.869 - 3.579k^2, \quad (31)$$

$$V_{S,{}^1G}(k^2) = 466.566, \quad (32)$$

$$V_{S,{}^3G}(k^2) = 0, \quad (33)$$

where we clearly see the violations of Wigner symmetry at short distances; that is, we only have

$$V_{{}^3L}(r) \sim V_{{}^1L}(r), \quad \text{even } L, \quad r \geqslant r_c. \quad (34)$$

This simple analysis suggests that Serber symmetry, when it works, holds to shorter distances than the Wigner symmetry. Our previous analysis in terms of mean phases [25] fully supports this fact. Indeed, higher partial waves with angular momentum l are necessarily small at small momenta owing to the well-known $\delta_l(p) \sim -\alpha_l p^{2l+1}$ threshold behavior. In fact, this is the case for $\delta_{{}^1P}$ and $\delta_{{}^1F}$. However, Serber symmetry implies that $\delta_{{}^3P}$ and $\delta_{{}^3F}$ are rather small not only in the threshold region but also in the entire elastic region, as can be clearly seen from Fig. 3.

C. Potentials and $V_{\text{low }k}$

A somewhat different perspective arises from a Wilsonian analysis of the NN interaction, which corresponds to a coarse graining of the potential. This viewpoint was implemented in Ref. [39], where the so-called $V_{\text{low }k}$ approach has been pursued, and corresponds to integrating out high-momentum modes below a given cutoff $k \leqslant \Lambda$ from the Lippmann-Schwinger equation. It was found that high-quality potential models (i.e., fitting the NN data to high accuracy and also incorporating OPE) collapse into a unique self-adjoint nonlocal potential for $\Lambda \sim 400$ MeV. This is a not a unreasonable result since all the potentials provide a rather satisfactory description of elastic NN scattering data up to $p \sim 400$ MeV. Moreover, the potential that emerges from eliminating high-energy modes can be accurately represented as the sum of the truncated original potential and a polynomial in the momentum [40],

$$V_{\text{low }k}(k', k) = V_{NN}(k', k) + V_{\text{CT}}^{\Lambda}(k', k), \quad (k, k') \leqslant \Lambda, \quad (35)$$

where $V_{NN}(k', k)$ is the original potential in momentum space for a given partial wave channel and $V_{\text{CT}}^{\Lambda}(k', k)$ is the effect of the high-energy states,

$$V_{\text{CT}}^{\Lambda}(k', k) = k^l k'^{l'} \left[C_0^{ll'}(\Lambda) + C_2^{ll'}(\Lambda)(k^2 + k'^2) + \cdots \right], \quad (36)$$

where the coefficients $C_n^{ll'}(\Lambda)$ play the role of counterterms. It should be noted that here $V_{NN}(k', k)$ is cut off *independent* of Λ whereas $V_{\text{CT}}^{\Lambda}(k', k)$ does depend on Λ. When the potential given by Eq. (35) is plugged into the truncated Lippmann-Schwinger equation (i.e., for intermediate states $q \leqslant \Lambda$), the phase shifts corresponding to the full original potential $V_{NN}(k', k)$ are reproduced. In Fig. 4 the corresponding diagonal $V_{\text{low }k}(p, p)$ mean potentials are plotted for

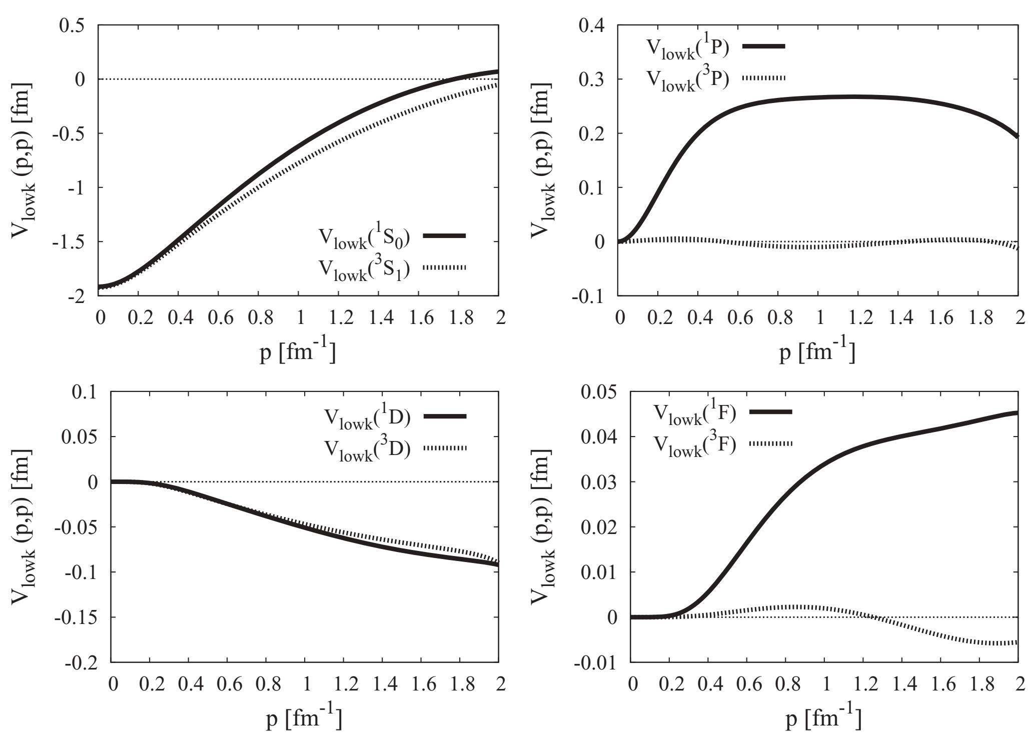

FIG. 4. Diagonal $V_{\text{low }k}(p, p)$ potentials (in femtometers) as a function of the momentum p (in fm^{-1}) for the Argonne-V18 [38], for the center of the Serber-Wigner multiplets. Wigner symmetry requires singlet and triplet potentials to coincide. Serber symmetry implies vanishing odd-L partial waves. Even-L waves possess Wigner symmetry whereas odd-L triplet waves exhibit Serber symmetry.

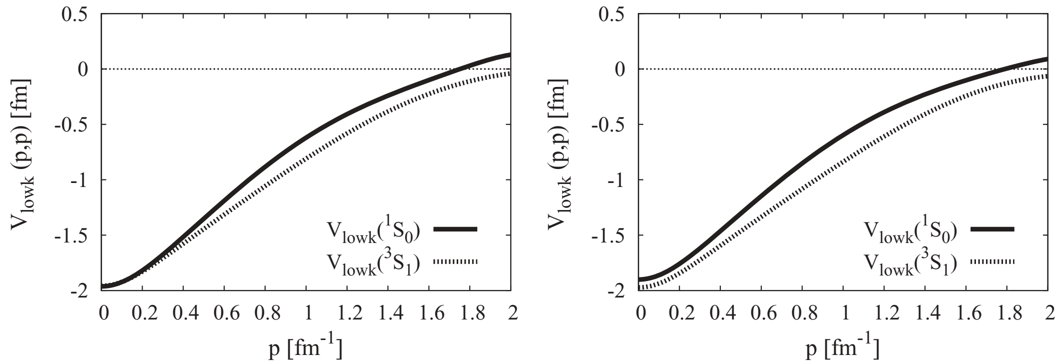

FIG. 5. Diagonal $V_{\mathrm{low}\,k}(p, p)$ potentials (in femtometers) as a function of the momentum p (in fm^{-1}) for the N^{3}LO-chiral potentials [45] for the S-wave states when the chiral cutoffs $\Lambda_\chi = 500$ MeV and $\Lambda_\chi = 600$ MeV are used. As we see there is a 5% violation of Wigner symmetry in the second case.

the Argonne-V18 force [38].[4] As we see both Wigner and Serber symmetries are, again, vividly evident. The important observation here is that the separation assumed by Eq. (35) does not manifestly display the symmetry. Actually, a more convenient representation would be to separate all polynomial dependence explicitly from the original potential

$$V_{\mathrm{low}\,k}(k', k) = \bar{V}_{NN}(k', k) + \bar{V}^{\Lambda}_{\mathrm{CT}}(k', k), \quad (k, k') \leqslant \Lambda, \quad (37)$$

so that if $\bar{V}^{\Lambda}_{\mathrm{CT}}(k', k)$ contains up to $\mathcal{O}(p^n)$ then $\bar{V}_{NN}(k', k)$ starts off at $\mathcal{O}(p^{n+1})$ (i.e., the next higher order). This way the departures from a pure polynomial may be viewed as true and explicit effects caused by the potential. In terms of these polynomials, Wigner and Serber symmetries are formulated from the coefficients

$$\bar{C}_0 = C_0 + C_0^{\mathrm{high}}(\Lambda) \quad (38)$$

constructed from the sum of the potential and the integrated-out contribution below a cutoff Λ, namely

$$\begin{aligned} \bar{C}_{0,{}^1L} &= \bar{C}_{0,{}^3L}, \qquad \text{even } L\,, \\ \bar{C}_{0,{}^3L} &= 0, \qquad \text{odd } L. \end{aligned} \quad (39)$$

It should be noted that the $V_{\mathrm{low}\,k}$ approach is in spirit nothing but the momentum space version of the PWA of the Nijmegen group in coordinate space where short distances, $r \leqslant r_c$, are integrated out and parametrized by means of an energy-dependent boundary condition. From this viewpoint the similarities as regards the Wigner and Serber symmetries are not surprising. This is why the standard boundary condition approach might also be denominated by $V_{\mathrm{high}\,R}$ (see also Ref. [41] for further discussion).

D. Chiral two-pion exchange

The chiral two-pion exchange (TPE) potentials computed in Refs. [42,43] using chiral perturbation theory (ChPT) are understood as direct consequences of the spontaneous chiral symmetry breaking in QCD. Actually, the TPE contribution takes over the OPE one at about $r = 2$ fm. At very long distances one has

$$V_{2\pi}^{\mathrm{ChPT}}(r) = (1 + 2\vec{\tau}_1 \cdot \vec{\tau}_2)\frac{e^{-2m_\pi r}}{r}\frac{3g_A^4 m_\pi^5}{1024 f_\pi^4 M_N \pi^2} + \cdots, \quad (40)$$

where m_π and M_N are the pion and nucleon masses, respectively, g_A is the axial coupling constant, and f_π is the pion weak decay constant. As we see Serber symmetry is broken already at long distances. Generally, these chiral potentials are supplemented by counterterms or equivalently boundary conditions when discussing NN scattering and generating phase shifts (see, e.g., Ref. [44]). Given that these NN phase shifts do fulfill the symmetry (see Fig. 3) we expect that the breaking of the symmetry at long distances must be compensated by the counterterms, which encode the unknown short-distance physics [44]. This can be verified by looking, for example, at the $V_{\mathrm{low}\,k}$ potential corresponding to the next-to-next-to-next-to-leading order (N^{3}LO) chiral potential, which contains its own cutoff parameter of $\Lambda_\chi = 500$ MeV [45]. This potential contains OPE and describes successfully the data and hence falls into the universality class of high-quality potentials [46] when the common $V_{\mathrm{low}\,k}$ cutoff scale $\Lambda = 400$ MeV is used. If the chiral potential is slightly detuned by taking $\Lambda_\chi = 600$ MeV one sees a low-momentum violation of the Wigner symmetry in Fig. 5 in total contradiction with the fact that one expects that asymptotically OPE should dominate. This shows that regarding the symmetry Λ_χ is fine-tuned. A more complete account of these issues will be presented elsewhere [47].

IV. ARE COUNTERTERMS FINGERPRINTS OF LONG-DISTANCE SYMMETRIES?

Given the fact that both Wigner and Serber symmetries can be interpreted as long-distance symmetries that roughly materialize at low energies in the potentials (see Fig. 2), the phase shifts (see Fig. 3), and the $V_{\mathrm{low}\,k}$ potentials (see Fig. 4) we find it appropriate to discuss how these results fit into renormalization ideas and the role played by the corresponding counterterms.

[4]We thank Scott K. Bogner for kindly providing the numbers of Ref. [40].

A. The perturbative point of view

As we have mentioned in the previous section, chiral potentials are generally used to describe NN scattering with the additional implementation of counterterms that cannot directly be determined from chiral symmetry alone. Nonetheless, one expects these counterterms to encode short-distance physics and hence to be related to the exchange of heavier mesonic degrees of freedom like those employed in the one-boson exchange (OBE) potentials [48]. The idea is quite naturally based on the resonance saturation hypothesis of the exchange forces (see, e.g., Ref. [49] for a discussion in the $\pi\pi$ scattering case). This is achieved by integrating out the heavy fields by using their classical equations of motion, and expanding the exchanged momentum between the nucleons as compared to the resonance mass case [50,51]. Schematically it corresponds to power expanding the Yukawa-like NN potentials as

$$\begin{aligned}\frac{g_M^2}{\mathbf{q}^2+M^2} &= \frac{g_M^2}{M^2} - \frac{g_M^2\mathbf{q^2}}{M^4} + \cdots \\ &= C_0 + C_2\left(\mathbf{p}^2+\mathbf{p}'^2\right) + C_1\mathbf{p}\cdot\mathbf{p}' + \cdots, \quad (41)\end{aligned}$$

where we are working in the CM system, we take the momentum transfer as $\mathbf{q}=\mathbf{p}-\mathbf{p}'$, and we ignore spin and isospin for simplicity. In this equation C_0 is an s-wave zero range, C_2 is an s-wave finite range, C_1 is a p wave, etc. More generally, Eq. (41) corresponds to a power series expansion of the potential in momentum space. Obviously, we expect such a procedure to be meaningful whenever the scattering process can be treated perturbatively (like, e.g., the case of peripheral waves). As is well known, central s waves cannot be treated perturbatively as the corresponding scattering amplitudes have poles very close to threshold, corresponding to a virtual state in the ${}^1S_0$ channel and the deuteron in the ${}^3S_1$-${}^3D_1$ channel. This does not mean, however, that the potential cannot be represented in the polynomial form of Eq. (41), but rather that the coefficients cannot be computed *directly* as the Fourier components of the potential.

B. The Wilsonian point of view

The momentum space $V_{\text{low}\,k}$ approach [40] makes clear that the long-distance behavior of the theory is not determined by the low-momentum components of the original potential *only*; one has to add virtual high-energy states, which also contribute to the interaction at low energies in the form of counterterms, as outlined by Eqs. (35) and (37). Alternatively, the more conventional coordinate space boundary condition (alias $V_{\text{high}\,R}$) method shows that the low-energy behavior of the theory is not determined *only* by the long-distance behavior of the potential; one has to include the contribution from integrated-out short distances in the form of boundary conditions. A true statement is that the low-momentum features of the interaction in the $V_{\text{low}\,k}(p,p)$ potential can be mapped into long-distance characteristics of the potential $V(r)$. The symmetries are formulated in terms of the conditions in Eq. (39).

C. Long-distance symmetries in nuclear potentials

To substantiate our points further, let us note that in Ref. [40] it was suggested that the $V_{\text{low}\,k}$ was a viable way of determining the effective interactions, which could be further used in shell-model calculations for finite nuclei. Actually, this interpretation when combined with our observation of Fig. 4 that Serber symmetry shows up quite universally has interesting consequences. Schematically, this can be implemented as a Skyrme-type effective (pseudo)potential [18]

$$\begin{aligned}V(\vec{r}) &= t_0(1+x_0P_\sigma)\delta^{(3)}(\vec{r}) + t_1(1+x_1P_\sigma)\{-\nabla^2,\delta^{(3)}(\vec{r})\} \\ &\quad - t_2(1+x_2P_\sigma)\nabla\delta^{(3)}(\vec{r})\nabla + \cdots, \quad (42)\end{aligned}$$

where $P_\sigma=(1+\sigma_1\cdot\sigma_2)/2$ is the spin exchange operator with $P_\sigma=-1$ for spin singlet $S=0$ and $P_\sigma=1$ for spin triplet $S=1$ states. The dots stand for spin-orbit, tensor interaction, etc. Of note is the close resemblance of the momentum space version of this potential

$$\begin{aligned}V(\mathbf{p}',\mathbf{p}) &= t_0(1+x_0P_\sigma) + t_1(1+x_1P_\sigma)(\mathbf{p}'^2+\mathbf{p}^2) \\ &\quad + t_2(1+x_2P_\sigma)\mathbf{p}'\cdot\mathbf{p} + \cdots \quad (43)\end{aligned}$$

to Eq. (37) after projection onto partial waves, where only S and P waves have been retained. Traditionally, binding energies have been used to determine the parameters t_i and x_i within a mean-field approach and many possible fits arise depending on the chosen observables (see, e.g., Ref. [19]) possibly displaying some spurious short-distance sensitivity beyond the range of applicability of Eq. (42). The low-momentum character of the Skyrme force suggests using the longest possible wavelength properties. Actually, inclusion of a tensor force and a new fitting strategy to single-particle energies [20] yields $x_2=-0.99$, which is an almost perfect Serber force for spin-triplets ($P_\sigma=1$) and reproduces the so-called SLy4 form of the Skyrme functional [19]. In light of our discussion this result seems quite natural as single-particle energies place attention in long wavelength states, a situation where $V_{\text{low}\,k}$ can be described by a pure polynomial in momentum [see Eq. (37)] and Serber symmetry becomes manifest *directly* from a coarse graining of the NN interaction.

D. Matching OBE potentials to chiral potentials

In Ref. [50] a systematic determination of counterterms has been carried out for a variety of realistic potentials that successfully fit the NN data by reading off the Fourier components of the potential [see, e.g., Eq. (41)]. The counterterms so obtained are then compared to those determined from direct fits to the NN data when the chiral potential is added. The spread of values for these counterterms found in Ref. [50] for realistic potentials, however, does not comply with the fact that all those potentials provide a quite satisfactory description of the phase shifts. Moreover, in Ref. [50] it is found that for the OBE Bonn potential [48]

$$C_{{}^1P} = +0.454\times10^{-4}\ \text{GeV}^{-4}, \quad (44)$$

$$C_{{}^3P} \equiv \tfrac{1}{9}\left(C_{{}^3P_0}+3C_{{}^3P_1}+5C_{{}^3P_2}\right) = -0.140\times10^{-4}\ \text{GeV}^{-4}. \quad (45)$$

Thus, the triplet to singlet ratio is $C_{^3P}/C_{^1P} \sim -0.33$ in this case. For the CD Bonn potential [52] one has $C_{^3P}/C_{^1P} \sim -0.7$ whereas Argonne AV-18 [38] yields $C_{^3P}/C_{^1P} \sim -0.54$. These large factors contrast with the much smaller factor $V_{S,^3P}(k^2)/V_{S,^1P}(k^2) \sim 1/10$ of the PWA sketched in Sec. III B. They also disagree with the almost vanishing ratio $V_{^3P}(p,p)/V_{^1P}(p,p)$ found for the $V_{\text{low }k}$ potentials described in Sec. III C, which yield a universal result (see also Fig. 4 for the particular AV-18 potential). The reason for this disagreement is that the correct formulation of the symmetry conditions is given by Eq. (39), which are made up from the potential plus the contribution of the high-energy tail. Thus, it appears that in the approach of Ref. [50] Serber symmetry is more strongly violated at short distances than is expected from other means. In our view the spread of values found in Ref. [50] might possibly reflect an inadequacy of the method used to characterize the long-distance coarse-grained NN dynamics where, as we have shown, Serber symmetry becomes quite accurate. Actually, the matching of counterterms between, say, the OBE potential and the chiral potentials is done in terms of objects that have a radically different large-N_c behavior (see Sec. V for further details). For instance, although $C_0^{\text{OBE}} \sim g_M^2/m_M^2 \sim N_c$ because $g_M \sim N_c^{\frac{1}{2}}$ and $m_M \sim N_c^0$ one has $C_0^{\text{chiral}} \sim g_A^4 m_\pi^2/f_\pi^4 \sim N_c^2$ since $m_\pi \sim N_c^0$, $f_\pi \sim N_c^{\frac{1}{2}}$ and $g_A \sim N_c$. In fact, the values of the counterterms determined from resonance exchange are generally *not* simply determined by the coefficients of the power series expansion of the potential in momentum space, as schematically given by Eq. (41), since they undergo renormalization and hence run with the scale.

E. Long-distance symmetry and off-shellness

The previous analysis shows that nothing forbids having a potential that breaks the symmetry strongly on the one hand and being able to *simultaneously* fit the scattering data that manifestly display the symmetry on the other hand. Actually, this can only be achieved by some degree of compensating symmetry violation between long and short distances.[5] However, it is somewhat unnatural as it does not reflect the true character of the theory and relegates the role of the symmetry to be an accidental one. As is widely accepted, unveiling symmetries is not mandatory but makes life much easier.[6]

Of course, these observations are true as long as we restrict ourselves to on-shell properties, such as NN scattering. However, would these symmetries have any consequence for off-shell nucleons? One may clearly have arbitrary short-distance parametrizations of the force without a sizable change of the phase shifts. However, the universality of long-distance potentials above $\sim$1.5 fm or, equivalently, a coarse graining of the interaction with the given length scale $\sim\pi/\Lambda$ such as $V_{\text{low }k}$ is *by definition* based on insensitivity to shorter wavelengths. Our discussion here on effective forces illustrates the fact that these redefinitions of the potential in the NN scattering problem *cannot* affect the effective force and so a violation of the Serber symmetry has a physical significance for wavelengths larger than the coarse-graining scale.

V. SERBER FORCE FROM A LARGE-N_c PERSPECTIVE

Up till now, in this paper we have provided evidence that long-distance symmetries such as Wigner's and Serber's do really take place in the two-nucleon system. From now on we are concerned with trying to determine whether those symmetries are purely accidental ones or whether they obey some pattern following more closely from QCD. Actually, we found [25] that the large-N_c limit [28,29] (for comprehensive reviews see, e.g., Refs. [30–32]) provides a rationale for Wigner symmetry. The fact that Serber symmetry holds when Wigner symmetry fails suggests analyzing the large-N_c consequences more thoroughly. Although we do not find a completely unique answer regarding the origin of Serber symmetry, the analysis does show interesting features, as will be discussed.

A. Large-N_c and long-distance symmetry

In this section we want to analyze these long-distance Serber and Wigner symmetries within the two-nucleon system from the large-N_c expansion [28,29] (for comprehensive reviews see, e.g., Refs. [30–32]). One feature of large N_c that becomes relevant for the NN problem is that is does not specially hold for long or short distances. This allows us in particular to switch from perturbative quarks and gluons at short distances to the nonperturbative hadrons, the degrees of freedom of interest to nuclear physics. This quark-hadron duality makes possible the applicability of large-N_c counting rules directly to baryon-meson interactions, at distances where explicit quark-gluon effects are not expected to be crucial. The procedure provides a set of consistency conditions from which the contracted SU(4) symmetry is deduced [30–32]. Thus, although the large-N_c scaling behavior and spin-flavor structure of the NN potential, Eq. (46), is directly established in terms of quarks and gluons [34], quark-hadron duality at distances larger than the confinement scale requires an identification of the corresponding exchanged mesons, and hence a link to the OBE potentials is provided. However, for internal consistency of the hadronic version of the large-N_c expansion, these counting rules should hold regardless of the number of exchanged mesons between the nucleons. Actually, naive power counting suggests huge violations of the NN counting rules. The issue has been clarified after the work of Banerjee, Cohen, and Gelman for all meson exchange cases with spin 0 and spin 1 [35] where the necessary cancellations between meson retardation in direct box diagrams and crossed

[5]This is the case for instance of chiral TPE potentials (see Sec. III D), where the potential [42,43] breaks the symmetry above 1.6 fm but the data can be described [44] with this truncated potential plus suitable energy-dependent boundary conditions.

[6]This discussion is somewhat similar to the use of regularization schemes in effective field theory; although it is possible to break the symmetry by all allowed counterterms, final physical results will depend on redundant combinations of parameters expressing the symmetry. In practice it is far more convenient to use a regularization scheme where the symmetry is manifestly preserved.

box diagrams was indeed shown to take place. In the TPE case the Δ isobar embodying the contracted SU(4) symmetry was explicitly needed. Although the exchange of three or more mesons appeared initially to present puzzling inconsistencies [53] a possible outcome was outlined in Ref. [54] by noting that large-N_c counting rules apply to energy-independent and hence self-adjoint potentials.

Before entering into a more detailed discussion one should be aware of the fact that strictly speaking the large-N_c picture for nuclei *does not look at all* like the physical world because of fine tuning of low-energy parameters. As already noted by Witten [29] baryons are solitons whose interactions are described by a time-dependent mean-field theory. A smooth large-N_c limit is possible if, besides being heavy, nucleons are also assumed to be fast; that is, their momentum scaling as $p \sim N_c$ resembles a time-dependent mean-field picture of elastic scattering of rapidly moving solitons, the consequences of which could hardly be tested experimentally. Furthermore, aside from spin and isospin there is no trace of quantum scattering effects. As noted by Cohen and co-workers [55,56], the leading equations have, in addition to the standard spin, isospin, parity, and angular momentum conservation laws, an extra and genuine large-N_c symmetry—the spin-isospin reversal of a single particle, $\sigma_i \to -\sigma_i$, $\tau_a \to -\tau_a$. Relations deduced from this spin-isospin reversal symmetry could be tested in a mean-field approximation in a regime where the momentum is still large, $p \sim \sqrt{N_c}$, but the kinetic energy, $p^2/M \sim N_c^0$, is small compared to the potential energy, $V \sim N_c$. Calculations of the maximal elastic energy in proton-neutron and proton-proton scattering for the spin asymmetry differential cross sections have been shown to fail, indicating a shortcoming of the leading N_c approximation for the NN interaction at least in the time-dependent mean-field version. The estimate of Ref. [56]—that corrections only scale as $1/\sqrt{N_c}$ and so are parametrically small but numerically large—may explain this failure. This negative result leaves little room for a successful mean-field large-N_c description of NN scattering and shows that a literal interpretation of large N_c is far different from the real $N_c = 3$ world. However, the components of the NN force may still follow a large-N_c hierarchy, which in the meson exchange picture determines the relative strength of meson-nucleon couplings. Actually, this is coherent within the long-distance symmetry scenario. In other words, whereas the potential may comply with a large-N_c scaling pattern, the renormalization conditions and, in particular, counterterms, need not follow the same pattern. Actually, the case of $^1S_0$ and $^3S_1$ channels with regard to Wigner symmetry corresponds to such a situation. From this viewpoint we analyze only large-N_c potentials and consider binding energy or scattering lengths as independent parameters, thus avoiding the fine-tuning problem [57].

B. Large-N_c NN components of the potential

One of the advantages of taking the large-N_c limit is that the nucleons become infinitely heavy, so if their momentum is taken to be fixed and N_c independent, $p \sim N_c^0$, the nonrelativistic potential is a well-defined object and presumably not subjected to the many ambiguities of relativistic potentials. This suggests a scheme departing from Witten's original proposal where smoothness is required for the quantum mechanical NN potential instead of the S matrix. Based on the contracted SU(4) large-N_c symmetry the spin-flavor structure of the NN interaction was analyzed by Kaplan, Savage, and Manohar [33,34], who found that the leading N_c nucleon-nucleon potential indeed scales as N_c and has the structure

$$V(r) = V_C(r) + \tau_1 \cdot \tau_2 \,[\sigma_1 \cdot \sigma_2 W_S(r) + S_{12} W_T(r)]\,. \quad (46)$$

It is noteworthy that the tensor force appears at the leading order in the large-N_c expansion. This only corresponds to the $NN \to NN$ component of the interaction. More generally, one should also at least consider $NN \to N\Delta$ and $NN \to \Delta\Delta$ processes as dynamical coupled channels that open up as soon as the nucleon and the Δ become degenerate since $M_\Delta - M_N \sim N_c^{-1}$. Note that in this limit *all* other parameters in the potential should also evolve with N_c. This is another example in which a literal interpretation of the large-N_c framework will most likely fail in a nuclear physics environment. The inclusion of $\Delta(1232)$ has been favored in the NN phenomenology [58]. One should, however, note the difference between having a potential that has a well-defined (although unrealistic) large-N_c limit from taking the large-N_c limit in the actual calculation (see Ref. [59]).[7]

From the large-N_c potential, Eq. (46), we have for the center of multiplet potentials the sum rules

$$\begin{aligned} V_{^1L} &= V_{^3L} = V_C(r) - 3W_S(r), \quad (-1)^L = +1, \\ V_{^1L} &= V_C(r) + 9W_S(r), \quad (-1)^L = -1, \\ V_{^3L} &= V_C(r) + \ W_S(r), \quad (-1)^L = -1, \end{aligned} \quad (47)$$

where, as we see, $V_{^1L} \neq V_{^3L}$ for odd L. Thus, large N_c *implies* Wigner symmetry in even-L channels and *allows* a violation of Wigner symmetry in odd-L partial waves while it *allows* a violation of Serber symmetry in spin singlet channels.[8] The question is whether or not large N_c *implies* Serber symmetry in spin triplet channels as we observe both for the potentials in Fig. 2 as well as for the phase shifts in Fig. 2. However, from the odd waves we see from Fig. 3 that the mean triplet phase is close to null; thus one might attribute this feature to an accidental symmetry where the odd waves potentials

[7]This difference is conceptually similar to the chiral perturbative setup of NN potentials [42–45] based on the smallness of the pion mass as compared to other scales; if the pion was massless the NN interaction would be a van der Waals (unrealistic) long-range potential $V(r) \sim 1/(M_N^m f_\pi^n r^{m+n+1})$. However, under renormalization with the *physical* scattering lengths, the $^1S_0$ and $^3S_1$ phases with TPE potentials in the chiral limit look rather reasonable (see Sec. VII in Ref. [60]).

[8]As noted in Ref. [57], Eq. (46) would suggest that this potential be renormalized by a contact interaction piece to be at least of the same form as the long-distance potentials, that is, $V_{\rm short}(\vec{x}) = (C_C + \tau_1 \cdot \tau_2[\sigma_1 \cdot \sigma_2 C_S + S_{12} C_T])\delta(\vec{x})$, which embodies a short-distance Wigner symmetry for S waves since $C_{^1S_0} = C_{^3S_1} = C_C - 3C_S$ and hence implies $\delta_{^1S_0} = \delta_{^3S_1}$. The long-distance symmetry interpretation [25] allows a *more general* structure $C_{^1S_0} \neq C_{^3S_1}$, explains why $\delta_{^1S_0} \neq \delta_{^3S_1}$, and avoids the extra spin-isospin reversal symmetry of a single particle, $\sigma_i \to -\sigma_i$, $\tau_a \to -\tau_a$ of Ref. [56].

are likewise negligible. In the large-N_c limit this means $V_C + 9W_S \gg V_C + W_S$, a fact that should be verified.

C. OBE large-N_c potentials

According to Refs. [33,34] in the leading large N_c one has $V_C \sim W_S \sim N_c$ whereas $V_S \sim W_C \sim 1/N_c$. To proceed further and gain some insight we write the potentials in terms of leading single-meson exchanges (see also Ref. [35]). The Yukawa-like potentials (in the notation of Ref. [48]) are

$$\begin{aligned} V_C(r) &= -\frac{g_{\sigma NN}^2}{4\pi}\frac{e^{-m_\sigma r}}{r} + \frac{g_{\omega NN}^2}{4\pi}\frac{e^{-m_\omega r}}{r}, \\ W_S(r) &= \frac{1}{12}\frac{g_{\pi NN}^2}{4\pi}\frac{m_\pi^2}{\Lambda_N^2}\frac{e^{-m_\pi r}}{r} + \frac{1}{6}\frac{f_{\rho NN}^2}{4\pi}\frac{m_\rho^2}{\Lambda_N^2}\frac{e^{-m_\rho r}}{r}, \end{aligned} \tag{48}$$

where $\Lambda_N = 3M_N/N_c$ is a scale that is numerically equal to the nucleon mass and is $\mathcal{O}(N_c^0)$. All meson couplings scale as $g_{\sigma NN}, g_{\pi NN}, g_{\omega NN}, f_{\rho NN} \sim \sqrt{N_c}$ whereas all meson masses scale as $m_\pi, m_\sigma, m_\rho, m_\omega \sim N_c^0$. In principle there would be infinitely many contributions but we stop at the vector mesons. A relevant question that will be postponed to the next section regards *what* values of Yukawa masses should one take. This is particularly relevant for the m_σ case. Note that the tensorial structure of the potential in Eq. (46) is complete to $\mathcal{O}(N_c^{-1})$. This leaves room for $\mathcal{O}(N_c^0)$ corrections to the NN potential *without* generating new dependencies triggered by subleading mass shifts $\Delta m_\sigma = \mathcal{O}(N_c^{-1})$ and subleading vertex corrections $\Delta g_{\sigma NN} = \mathcal{O}(N_c^{-1/2})$.

As we have already mentioned, to obtain Serber symmetry we must get a large cancellation. At short distances the Yukawa OBE potentials have Coulomb-like behavior, $V \to C/(4\pi r)$, with the dimensionless combinations

$$C_{V_C+W_S} = -g_{\sigma NN}^2 + g_{\omega NN}^2 + \frac{f_{\rho NN}^2 m_\rho^2}{6M_N^2}, \tag{49}$$

$$C_{V_C+9W_S} = -g_{\sigma NN}^2 + g_{\omega NN}^2 + \frac{3f_{\rho NN}^2 m_\rho^2}{2M_N^2}, \tag{50}$$

where the small OPE contribution has been dropped. To resemble Serber symmetry we should have $C_{V_C+W_S} \ll C_{V_C+9W_S}$. There are several scenarios where this can be achieved. For instance, if we impose the OPE 1/9 rule for the full potential we have $g_{\sigma NN}^2 = g_{\omega NN}^2$. Using SU(3), $3g_{\rho NN} = g_{\omega NN}$, Sakurai's universality $g_{\rho NN} = g_{\rho\pi\pi}/2$, the current-algebra KSFR relation, $\sqrt{2}g_{\rho\pi\pi} f_\pi = m_\rho$, and the scalar Goldberger-Treiman relation, $g_{\sigma NN} f_\pi = M_N$, one would get $M_N = N_c m_\rho/(2\sqrt{2})$, a not unreasonable result. This only addresses the cancellation at short distances. The cancellation would be more effective at intermediate distances if m_ρ and m_σ would be numerically closer. In this regard, let us note that there are various schemes where an identity between scalar and vector meson masses can be explicitly verified [61–63]. In reality, however, the scalar and vector masses are sufficiently different ($m_\sigma = 444$ MeV versus $m_\rho = 770$ MeV). In the next section we want to analyze this apparent contradiction.

VI. FROM $\pi\pi$ RESONANCES TO NN YUKAWA POTENTIALS

A. Correlated two-pion exchange

As we have already mentioned TPE is a genuine test of chiral symmetry. However, it is well known that the iterated exchange of two pions may become in the t channel either a σ or a ρ resonance for isoscalar and isovector states, respectively. Although the interactions leading to this collectiveness are controlled to a great extent by chiral symmetry [64–66], the resulting contributions to the NN potential in terms of boson exchanges bear a very indirect relation to it. The relation of the ubiquitous scalar meson in nuclear physics and NN forces in terms of correlated two-pion exchange has been pointed out many times [48,67–69] (see, e.g., Refs. [42,70–72] for a discussion in a chiral context). Attempts to introduce chiral Lagrangeans in nuclear physics have been numerous [73–75] but the implications for the OBE potential are meager despite the fact that useful relations among couplings can be deduced.[9] As we will see, they provide complementary information to the large-N_c requirements.

Note that the leading term generating the scalar meson is $g_A^4/f_\pi^6 \sim N_c$ but it occurs first at N^{3}LO in the chiral counting. The central potential reads [42,70–72]

$$V_{NN}^C(r) = -\frac{32\pi}{3m_\pi^4}\int \frac{d^3q}{(2\pi)^3} e^{iq\cdot x}[\sigma_{\pi N}(-q^2)]^2 t_{00}(-q^2), \tag{51}$$

where $\sigma_{\pi N}(s)$ is the πN sigma term and $t_{00}(s)$ is the $\pi\pi$ scattering amplitude in the $I = J = 0$ channel as a function of the $\pi\pi$ CM energy $\sqrt{s}$ [see also Eq. (53)]. Under the inclusion of Δ resonance contributions, Eq. (51) is modified by an additive redefinition of $\sigma_{\pi N}$ to include those Δ states [70]. In the large-N_c limit, $t_{\pi\pi}(s) \sim 1/N_c$ whereas $\sigma_{\pi N}(s) \sim N_c$, yielding $V_{NN} \sim N_c$ as expected [34]. Actually, at the sigma pole

$$\frac{32\pi}{3m_\pi^4}[\sigma_{\pi N}(s)]^2 t_{\pi\pi}^{II}(s) \to \frac{g_{\sigma NN}^2}{s-(m_\sigma - i\Gamma_\sigma/2)^2} \to \frac{g_{\sigma NN}^2}{s-m_\sigma^2}, \tag{52}$$

where in the second step we have taken the large-N_c limit. This yields $g_{\sigma\pi\pi} \sim 1/\sqrt{N_c}$, provided $m_\sigma \sim N_c^0$ and $\Gamma_\sigma \sim 1/N_c$. The "fictitious" narrow σ exchange has been attributed to $N\Delta + \Delta\Delta$ intermediate states [42], to 2π iterated pions [72], or to both [70]. This identification is based on fitting the resulting r-space potentials to a Yukawa function in a *reasonable* distance range.

B. Exchange of pole resonances

In this section we separate the resonance contribution to the NN potential from the background, neglecting for simplicity the vertex correction in Eq. (51). The most obvious definition

[9] We should mention the Goldberger-Treimann relations for pions, $g_A M_N = g_{\pi NN} f_\pi$, and scalars, $M_N = g_{\sigma NN} f_\pi$, which yield $g_{\pi NN} = 12.8$ and $g_{\sigma NN} = 10.1$, and the KSFR-universality relation, which yields $g_{\rho NN} = g_{\rho\pi\pi}/2 = m_\rho/f_\pi/\sqrt{8} = 2.9$.

of the σ or ρ propagator is via the $\pi\pi$ scattering amplitude in the scalar-isoscalar and vector-isovector channels, $(J, I) = (0, 0)$ and $(J, I) = (1, 1)$, respectively. We use the definition

$$t_{IJ}(s) = \frac{1}{2i\rho_{\pi\pi}(s)}(e^{2i\delta_{IJ}(s)} - 1), \tag{53}$$

with $\rho_{\pi\pi}(s) = \sqrt{1 - 4m_\pi^2/s}$ as the phase space in our notation. We take into account the fact that on the second Riemann sheet (taking σ as an example) the amplitude has a pole

$$t_{00}^{\mathrm{II}}(s) \to \frac{R_\sigma}{s - s_\sigma}, \tag{54}$$

with $\sqrt{s_\sigma} = M_\sigma - i\Gamma_\sigma/2$ as the pole position and R_σ the corresponding residue. Here we define, as usual, the analytical continuation as

$$t_{00}^{\mathrm{II}}(z)^{-1} - t_{00}^{\mathrm{I}}(z)^{-1} = 2i\rho_{\pi\pi}(z). \tag{55}$$

By continuity $t_{00}(s) \equiv t_{00}^{\mathrm{I}}(s \pm i0^+) = t_{00}^{\mathrm{II}}(s \mp i0^+)$ and thus unitarity requires $\rho_{\pi\pi}(s + i0^+) = -\rho_{\pi\pi}(s - i0^+)$. One has for the (suitably normalized) scalar propagator

$$D_S(s) = \frac{t_{00}(s)}{|R_\sigma|}, \tag{56}$$

in the whole complex plane. In particular,

$$D_S^{\mathrm{II}}(s) = \frac{t_{00}^{\mathrm{II}}(s)}{|R_\sigma|} \to \frac{e^{i\varphi_\sigma}}{s - (M_\sigma - i\Gamma_\sigma/2)^2}, \tag{57}$$

where the phase φ_σ is defined as $e^{i\varphi_\sigma} = R_\sigma/|R_\sigma|$ and is related to the background (i.e., the nonpole contribution). In Appendix A we discuss a toy model for $\pi\pi$ scattering [76] that proves quite useful to fix ideas. The function $D_S(s)$ is analytic in the complex s-plane with a 2π right cut along the $(4m_\pi^2, \infty)$ line stemming from unitarity in $\pi\pi$ scattering and a left cut running from $(-\infty, 0)$ owing to particle exchange in the u and t channels. If we assume that the scattering amplitude is proportional to this propagator the corresponding $\pi\pi$ phase shift is then given by

$$e^{2i\delta_{00}(s)} = \frac{t_{00}(s + i0^+)}{t_{00}(s - i0^+)} = \frac{D_S(s + i0^+)}{D_S(s - i0^+)}. \tag{58}$$

The propagator satisfies the unsubtracted dispersion relation [77],

$$D_S(q^2) = \int_{4m_\pi^2}^{\infty} d\mu^2 \frac{\rho_S(\mu^2)}{\mu^2 - q^2}, \tag{59}$$

where the spectral function is related to the discontinuity across the unitarity branch cut[10]

$$\rho_S(s) = \frac{1}{2i\pi}\mathrm{Disc}\, D_S(s + i0^+) \tag{60}$$

$$= \frac{1}{\pi|R_\sigma|}\rho_{\pi\pi}(s)|t_{00}(s)|^2, \tag{61}$$

which satisfies the normalization condition

$$\int_{4m_\pi^2}^{\infty} d\mu^2 \rho_S(\mu^2) = Z_\sigma, \tag{62}$$

[10] The cut is defined as $\mathrm{Disc}\, t(s + i0^+) = t(s + i0^+) - t(s - i0^+) = 2i\,\mathrm{Im}\, t(s)$ for a real function below $\pi\pi$ threshold, $0 < s < 4m^2$.

where Z_σ is the integrated strength. Thus, the Fourier transformation of the propagator is

$$D_S(r) = \int \frac{d^3q}{(2\pi)^3} e^{i\vec{q}\cdot\vec{x}} D_S(-\vec{q}^{\,2})$$

$$= -\frac{1}{4\pi r}\int_{4m_\pi^2}^{\infty} d\mu^2 \rho_S(\mu^2) e^{-\mu r}. \tag{63}$$

According to Eq. (62), $D_S(r) \sim -Z_\sigma/(4\pi r)$ for small distances. We define the analytic function $\rho_S(z)e^{-\sqrt{z}r}$ for $r > 0$ in the cut plane without $(-\infty, 0)$ and $(4m_\pi^2, \infty)$ where

$$\rho_S(z) = \frac{1}{\pi|R_\sigma|}\rho_{\pi\pi}(z) t_{00}^{\mathrm{I}}(z) t_{00}^{\mathrm{II}}(z), \tag{64}$$

and fulfilling the boundary value condition $\rho_S(s) \equiv \rho_S(s + i0^+)$. This function has a pole at the complex point $z = s_\sigma = (M_\sigma - i\Gamma_\sigma/2)^2$ and a square-root branch cut at $z = 4m_\pi^2$ triggered by the phase space factor only since $t_{00}^{\mathrm{I}}(z)t_{00}^{\mathrm{II}}(z)$ is continuous, so that $\rho_S(s + i0^+) = -\rho_S(s - i0^+)$. Thus, we can write the spectral integral, Eq. (63), as running below the unitarity cut and by suitably deforming the contour in the fourth quadrant in the second Riemann sheet, as shown in Fig. 6, we can separate explicitly the contribution from the pole and the 2π background, yielding

$$D_S(r) = D_\sigma(r) + D_{2\pi}(r). \tag{65}$$

In principle, both contributions are complex, but the total result must be real and their imaginary parts must cancel identically (see Appendix A for a specific example). Because Eq. (55) implies $2it_{00}^{I}(s_\sigma)\rho_{\pi\pi}(s_\sigma) = 1$ the σ-pole contribution is effectively given by

$$\mathrm{Re}D_\sigma(r) = -\frac{Z_\sigma e^{-M_\sigma r}}{4\pi r}\left[\cos\left(\frac{r\Gamma_\sigma}{2}\right) - \tan\varphi_\sigma \sin\left(\frac{r\Gamma_\sigma}{2}\right)\right], \tag{66}$$

which is an oscillating function damped by an exponential. In the narrow-resonance limit, $\Gamma_\sigma \to 0$, one has $\varphi_\sigma = \mathcal{O}(\Gamma_\sigma)$, yielding

$$\mathrm{Re}D_\sigma(r) \sim -\frac{Z_\sigma e^{-M_\sigma r}}{4\pi r}\left[1 + \mathcal{O}\left(\Gamma_\sigma^2\right)\right], \tag{67}$$

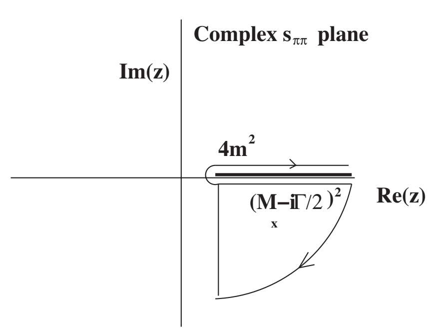

FIG. 6. $\pi\pi$ complex squared CM energy plane, showing the contour used in the main text yielding the pole+background decomposition for the coordinate space scalar-isoscalar propagator in Eq. (65).

which is a Yukawa potential. The 2π background reads

$$\text{Re } D_{2\pi}(r) = -\frac{1}{4\pi r}\frac{i}{2}\left[\int_0^\infty dy\rho_S\left(4m_\pi^2 - iy\right) e^{-r\sqrt{4m_\pi^2-iy}} - \int_0^\infty dy\rho_S\left(4m_\pi^2 + iy\right) e^{-r\sqrt{4m_\pi^2+iy}}\right]. \quad (68)$$

At large distances the integral is dominated by the small-y region, and we get the distinct TPE behavior $\sim e^{-2m_\pi r}$. The prefactor is obtained by expanding at small y and using the fact that unitarity imposes the spectral density to be proportional to the phase space factor, Eq. (61). Close to threshold, $s \to 4m_\pi^2$, involves the $\pi\pi$ scattering length a_{00} defined as $\delta_{00}(s) \sim a_{00}\sqrt{s-4m_\pi^2}$, yielding

$$\rho_S(s) = \frac{2m_\pi a_{00}^2}{\pi|R_\sigma|}\sqrt{s-4m_\pi^2} + \cdots. \quad (69)$$

We therefore get

$$D_{2\pi}(r) = -\frac{K_2(2m_\pi r)}{r^2}\frac{4m_\pi^3 a_{00}^2}{\pi^2|R_\sigma|} + \cdots \sim -\frac{e^{-2m_\pi r}}{r^{\frac{5}{2}}}\frac{2a_{00}^2 m_\pi^{\frac{5}{2}}}{\pi|R_\sigma|}. \quad (70)$$

In Appendix A the pole-background decomposition in Eq. (65) is checked explicitly in a toy model. The resonance contribution saturates the normalization completely with the 2π continuum background, yielding a vanishing contribution to the integrated strength. However, the resonance produces a Yukawa tail with an oscillatory modulation that alternates between attraction and repulsion, although the region where the oscillation is relevant depends largely on φ_σ.

C. $\pi\pi$ resonances at large N_c

The large-N_c analysis also opens up the possibility for a better understanding of the role played by the ubiquitous scalar meson. This is an essential ingredient, accounting phenomenologically for the mid-range nuclear attraction, and which, with a mass of $\sim$500 MeV, was originally proposed in the 1950s [78] to provide saturation and binding in nuclei. Over the years, there has always been some arbitrariness on the "effective" or "fictitious" scalar meson mass and coupling constant to the nucleon, partly stimulated by lack of other sources of information.[11] During the past decade, the situation has steadily changed, finally culminating, through the insistence and efforts of theoreticians [79], with the inclusion of the 0^{++} resonance (commonly denoted by σ) in the PDG [80] as the $f_0(600)$ seen as a $\pi\pi$ resonance, with a wide spread of values ranging from 400 to 1200 MeV for the mass and from 600 to 1200 MeV for the width [81]. These uncertainties have recently been sharpened by a benchmark determination based on Roy equations and chiral symmetry [36], yielding the value $m_\sigma - i\Gamma_\sigma/2 = 441^{+16}_{-8} - i272^{+9}_{-12}$ MeV. Once the formerly fictitious sigma became a real and well-determined lowest resonance of the QCD spectrum it became mandatory to analyze its consequences all over. Clearly, these numbers represent the value for $N_c = 3$, but large-N_c counting requires that for mesons $m_\sigma \sim N_c^0$ and $\Gamma_\sigma \sim 1/N_c$.

In this regard the large-N_c analysis may provide a clue to *what* value should be taken for the σ mass [82].[12] Of course, similar remarks apply to the width of other mesons, such as the ρ, as well. If we make use of the large-N_c expansion according to the standard assumption ($M^{(k)} \sim N_c^{-k}$)

$$M_\sigma = M_\sigma^{(0)} + M_\sigma^{(1)} + \mathcal{O}\left(N_c^{-2}\right), \quad (71)$$

$$\Gamma_\sigma = \Gamma_\sigma^{(1)} + \mathcal{O}\left(N_c^{-2}\right), \quad (72)$$

the pole contribution becomes

$$D_\sigma(r) = -\frac{e^{-m_\sigma r}}{4\pi r} + \mathcal{O}\left(N_c^{-2}\right), \quad (73)$$

where $m_\sigma = M_\sigma^{(0)} + M_\sigma^{(1)}$, representing the resonance mass to NLO in the $1/N_c$ expansion, should be used. Note that the width does not contribute to this order. Thus, for all purposes we may use a Yukawa potential to represent the exchange of a resonance. However, what *numerical* value of this m_σ should one use for the NN problem? Model calculations based on N_c scaling of $\pi\pi$ chiral unitary phase shifts for $N_c = 3$ suggest sizable modifications as compared with the accurately determined pole position when N_c is varied but the numerical results are not very robust [85].[13] From an

[11] For instance, in the very successful charge-dependent (CD) Bonn potential [52] any partial wave $^{2S+1}L_J$-channel is fitted with a different scalar meson mass and coupling.

[12] Large-N_c studies in $\pi\pi$ scattering based on scaling and unitarization with the inverse amplitude method (IAM) of ChPT amplitudes provide results that regarding the troublesome scalar meson depend on details of the scheme used. Although the one-loop coupled channel approach [83] yields any possible m_σ and a large width (in apparent contradiction with standard large-N_c counting [28,29]), the (presumably more reliable) two-loop approach [84] yields a large mass shift (by a factor of 2) for the scalar meson when going from $N_c = 3$ to $N_c = \infty$, yielding $m_\sigma \to 900$ MeV, but a small shift in the case of the ρ meson. One should note the large uncertainties of the two-loop IAM method documented in Ref. [66]. Based on the Bethe-Salpeter approach to lowest order [65] we have estimated $m_\sigma \to 500$ MeV [82]. In Ref. [85] it is argued that $m_\sigma \to m_\rho$ from the one-loop IAM.

[13] Actually, according to Ref. [86] the effect of a meson width in the Yukawa-like potential is

$$V(r) = -\frac{g^2}{4\pi}\left(1 - \frac{\Gamma_\sigma}{m_\sigma \pi}\right) e^{-(m_\sigma + \Gamma_\sigma/\pi)r},$$

which corresponds to a NLO large-N_c renormalization of the mass and coupling and provides an $\mathcal{O}(N_c^0)$ correction to the central potential. The analysis is based on separating the integrand into different intervals that become dominant at large distances. Our analysis separates first the pole contribution from the background and then studies each contribution separately. We note, however, that one can extract a Yukawa potential of the meson even for the large and physical width in the region where the potential is operating with quite sensible values [76]. In Appendix B we update this analysis using recent parametrizations of $\pi\pi$ scattering provided in Refs. [87,88], confirming the Yukawa behavior. The main reason for this behavior is that the potential is being probed for spacelike exchanged four-momentum, whereas the resonance behavior takes place in the timelike region corresponding to the crossed process $\bar{N}N \to 2\pi$.

alternative viewpoint, to the same accuracy, the large-N_c NLO pole contribution could be replaced by the equivalent Breit-Wigner resonance mass to the same approximation, since according to Ref. [85] we may take

$$\delta_{00}\left(m_\sigma^2\right) = \frac{\pi}{2} + \mathcal{O}\left(1/N_c^3\right). \tag{74}$$

Thus, at leading and next-to-leading orders in the large-N_c limit the exchange of a resonance between nucleons can be represented at long distances as a Yukawa potential with the Breit-Wigner mass to $\mathcal{O}(N_c^{-2})$. The vertex correction $\sigma_{\pi N}$ [see, e.g., Eq. (51)] just adds a coupling constant, yielding

$$V_\sigma(r) = -\frac{g_{\sigma NN}^2}{4\pi}\frac{e^{-m_\sigma r}}{r} + \mathcal{O}(1/N_c). \tag{75}$$

Of course, the same type of arguments apply to the ρ-meson exchange, with the only modification

$$\delta_{11}\left(m_\rho^2\right) = \frac{\pi}{2} + \mathcal{O}\left(1/N_c^3\right), \tag{76}$$

where now $m_\rho = M_\rho^{(0)} + M_\rho^{(1)}$. In Fig. 7 we show the data for $\pi\pi$ phase shifts, where we see that the *true* Breit-Wigner masses are not very different. Of course, these arguments do not imply that the Yukawa masses should *exactly* coincide, but at least they suggest that one should expect a large shift for the σ mass from the pole position and a very small one for the ρ meson mass when the next-to-leading $1/N_c$ correction to the pole masses are considered. The identity of scalar and vector masses has been deduced from several scenarios based on algebraic chiral symmetry [61,89]. Actually, it has been shown that $m_\rho = m_\sigma$ *without* appealing to the strict large-N_c limit but assuming the narrow resonance approximation (see also Ref. [90]). A recent analysis [91] also supports this result.

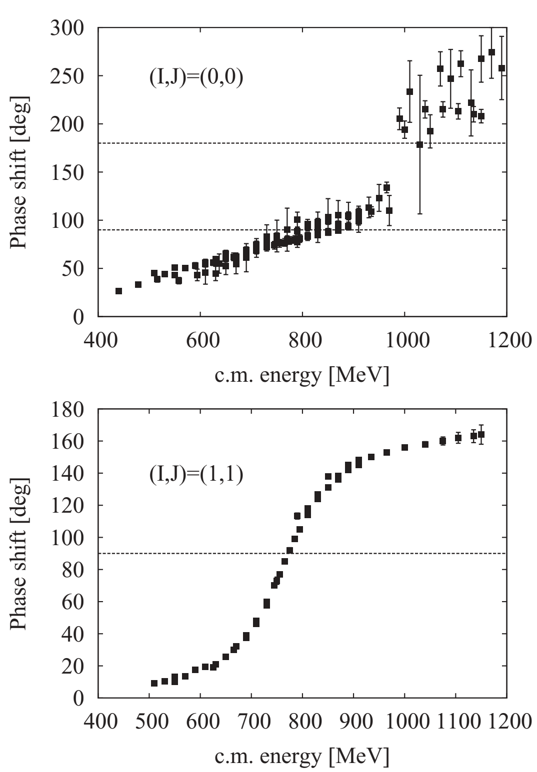

FIG. 7. $\pi\pi$ scattering phase shifts (in degrees) as a function of the CM energy $\sqrt{s}$. Horizontal lines mark the position of the Breit-Wigner resonances. Data are from Refs. [92–98].

VII. CONCLUSIONS

Serber symmetry seems to be an evident but puzzling symmetry of the NN system. Since it was proposed more than 60 years ago no clear explanation based on the more fundamental QCD Lagrangean has been put forward.

In the present paper we have analyzed the problem from the viewpoint of *long-distance symmetries*, a concept that has proven useful in the study of Wigner SU(4) spin-flavor symmetry. Actually, Serber symmetry is clearly seen in the np differential cross section, implying a set of sum rules for the partial wave phase shifts that are well verified to a few percent level in the entire elastic region. Although this situation corresponds to scattering of on-shell nucleons, it would be rather interesting to establish the symmetry beyond this case. Therefore, we have formulated these sum rules at the level of high-quality potentials (i.e., potentials that describe elastic NN scattering with $\chi^2/\mathrm{DOF} \sim 1$) that are also well verified at distances above 1 fm. This suggests that a coarse graining of the NN interaction might also display the symmetry. The equivalent momentum-space Wilsonian viewpoint is implemented explicitly by the $V_{\mathrm{low}\,k}$ approach by integrating all modes below a certain cutoff $\Lambda \sim 400$. By analyzing existing $V_{\mathrm{low}\,k}$ calculations for high-quality potentials we have shown that Serber symmetry is indeed fulfilled to a high degree. We recall that within the $V_{\mathrm{low}\,k}$ approach this symmetry has direct implications in shell-model calculations for finite nuclei since the $V_{\mathrm{low}\,k}$ potential corresponds to the effective nuclear interaction.

A surprising finding of the present paper is that chiral potentials, although implementing extremely important QCD features, do not fulfill the symmetry to the same degree as current high-quality potentials. This effect must necessarily be compensated by similar symmetry violations in the counterterms encoding the nonchiral and unknown short-distance interaction and needed to describe NN phase shifts where the symmetry does indeed happen. This is not necessarily a deficiency of the chiral approach but it is disturbing that the symmetry does not manifest at long distances, unlike high-quality potentials. This may be a general feature of chiral potentials that requires further investigation [47].

In an attempt to provide a more fundamental understanding of the striking but so far accidental Serber symmetry, we have also speculated how it might arise from QCD within the large-N_c perspective in the second part of the paper. The justification for advocating such a possible playground is threefold. First, the NN potential tensorial structure is determined with a relative $1/N_c^2$ accuracy, which naively suggests a bold 10%. Second, the meson exchange picture is justified. Finally, we have found previously that such an expansion provides a rationale for the equally accidental and pre-QCD Wigner SU(4) symmetry. Actually, we found that large N_c predicts the NN channels where Wigner symmetry indeed works and fails phenomenologically. The very interpretation of Wigner symmetry as a long-distance symmetry suggests that at best we can only interpret this large-N_c prediction in a restrictive sense, i.e., as a feature of potentials and not of the S matrix. The intriguing point is that when Wigner symmetry fails, as allowed by large-N_c considerations, Serber symmetry holds instead. In the present paper we have verified the previous statements at the level of potentials at large distances or using $V_{\mathrm{low}\,k}$ potentials, reinforcing our previous conclusions based on just a pure phase shift analysis. Under those circumstances, it is therefore natural to analyze to what extent and even whether Serber symmetry could be justified at all from a large-N_c viewpoint. In practical terms we have shown that within a one-boson exchange framework, the fulfillment of the symmetry at the potential level is closely related to having not too dissimilar values of σ and ρ meson masses as they appear in Yukawa potentials. Actually, these σ and ρ states are associated with resonances that are seen in $\pi\pi$ scattering and can be uniquely defined as poles in the second Riemann sheet of the scattering amplitude at the invariant mass $\sqrt{s} = M_R - i\Gamma_R/2$. We have therefore analyzed the meaning of those resonances within the large-N_c picture, by assuming the standard mass $m_R \sim N_c^0$ and width $\Gamma_R \sim 1/N_c$ scaling. We have found that, provided we keep terms in the potential to NLO, meson widths do not contribute to the NN potential, as they are $\mathcal{O}(N_c^{-1})$ (i.e., a relative $1/N_c^2$ correction to the leading-order contribution). This justifies using a Yukawa potential where the mass corresponds to an approximation to the pole mass $m_R = M_R^{(0)} + M_R^{(1)}$, which cannot be distinguished from the Breit-Wigner mass up to $\mathcal{O}(N_c^{-2})$. This suggests that the masses m_σ and m_ρ that appear in the OBE potential could be interpreted as an approximation to the pole mass rather than its exact value. This supports the customary two-Yukawa representation of complex-pole resonances pursued in phenomenological approaches since it was first proposed [76], because in practice only the lowest Yukawa mass contributes significantly. The question of *what* numerical value should be used for the Yukawa mass is a difficult one, and at present we know of no other direct way than NN scattering fits, for which $m_\sigma = 501(25)$ MeV might be acceptable [99] when the uncorrelated 2π contribution is disregarded.

On a more fundamental level, however, lattice QCD calculations at variable N_c values (see, e.g., Ref. [100] for a review) might reliably determine the Yukawa mass parameters appearing in the large-N_c potential. A recent quenched QCD lattice calculation yields [101] $m_\rho/\sqrt{\sigma} = 1.670(24) - 0.22(23)/N_c^2$ with $\sqrt{\sigma}$ the string tension, which for $\sqrt{\sigma} = 444$ MeV yields $m_\rho = 740$ MeV for $m_\pi = 0$ (see also Ref. [102]). The extension of those calculations to compute the needed $1/N_c$ mass shift would be most welcome and would require full dynamical quarks. One should not forget that Serber symmetry holds to great accuracy in the real $N_c = 3$ world, and in this sense it represents a stringent test to lattice QCD calculations in P waves in the mid-range region. Amazingly, the only existing S-wave potential calculation [23] displays Wigner symmetry quite accurately.

Of course, although the numerical large-N_c similarity between scalar and vector meson masses could explain the observed Serber symmetry a truly accidental origin cannot be completely excluded. In any case the large-N_c form of the potential specified by Eq. (46) can be retained with relative $1/N_c^2$ accuracy since meson widths enter beyond that accuracy as subleading corrections, on equal footing with many other effects (spin-orbit, relativistic, and those from other mesons), independently of the size of the σ width for $N_c = 3$. A more satisfactory description could be achieved if one incorporates the coupling of $N\Delta$ and $\Delta\Delta$ channels, which remain closed in the real world for NN scattering below the pion production threshold but open up as soon as the Δ resonance becomes degenerate with the nucleon since $M_\Delta - M_N \sim N_c^{-1}$. These findings suggest pursuing a deeper and more quantitative analysis, but it remains to be seen whether the condition of reproducing a large-N_c behavior does indeed impose a useful constraint for the NN interaction in the real world with $N_c = 3$.

ACKNOWLEDGMENTS

We gratefully acknowledge Manuel Pavón Valderrama for a critical reading of the manuscript, Juan Nieves, Lorenzo Luis Salcedo, and José Ramón Peláez for discussions, and Scott K. Bogner for kindly providing the data corresponding to the V18 potentials of Ref. [39]. We also thank Jacek Dobaczewski and Rup Machleidt for useful communications. This work has been partially supported by the Spanish DGI and FEDER funds with Grant No. FIS2008-01143/FIS, Junta de Andalucía Grant No. FQM225-05, and EU Integrated Infrastructure Initiative Hadron Physics Project Contract No. RII3-CT-2004-506078.

APPENDIX A: TOY MODEL FOR $\pi\pi$ SCATTERING

In this Appendix we illustrate with a specific example our discussion of Sec. VI and in particular the pole-background decomposition of Eq. (65). According to Ref. [76] the finite width of the scalar meson can be modeled by the propagator

$$D_S(s) = \frac{1}{s - m_\sigma^2 - i m_\sigma \gamma_\sigma \sqrt{\frac{s-4m_\pi^2}{m_\sigma^2-4m_\pi^2}}}, \tag{A1}$$

for $t \geqslant 4m_\pi^2$. Below the elastic scattering threshold we use the standard definition $\sqrt{t - 4m_\pi^2} = -i\sqrt{|t - 4m_\pi^2|}e^{i\theta}$, where $0 \leqslant \theta = \mathrm{Arg}(t - 4m_\pi^2) < 2\pi$. This defines the propagator in the first Riemann sheet; the second Riemann sheet is determined from the usual continuity equation $D_S^{\mathrm{II}}(s + i0^+) = D_S^{\mathrm{I}}(s - i0^+)$. The pole position is given by

$$s_\sigma = (M_\sigma - i\Gamma_\sigma/2)^2 = m_\sigma^2 - \frac{\gamma_\sigma^2 m_\sigma^2}{2m_\sigma^2 - 8m_\pi^2} - i\,\frac{\gamma_\sigma m_\sigma \sqrt{4\left(m_\sigma^2 - 4m_\pi^2\right)^2 - \gamma_\sigma^2 m_\sigma^2}}{2m_\sigma^2 - 8m_\pi^2}. \tag{A2}$$

In the small-width limit the position of the pole and width are

$$M_\sigma = m_\sigma - \frac{\gamma_\sigma^2}{8m_\sigma}\frac{m_\sigma^2 + 4m_\pi^2}{m_\sigma^2 - 4m_\pi^2} + \mathcal{O}\left(\gamma_\sigma^4\right), \tag{A3}$$

$$\Gamma_\sigma = \gamma_\sigma + \mathcal{O}\left(\gamma_\sigma^3\right). \tag{A4}$$

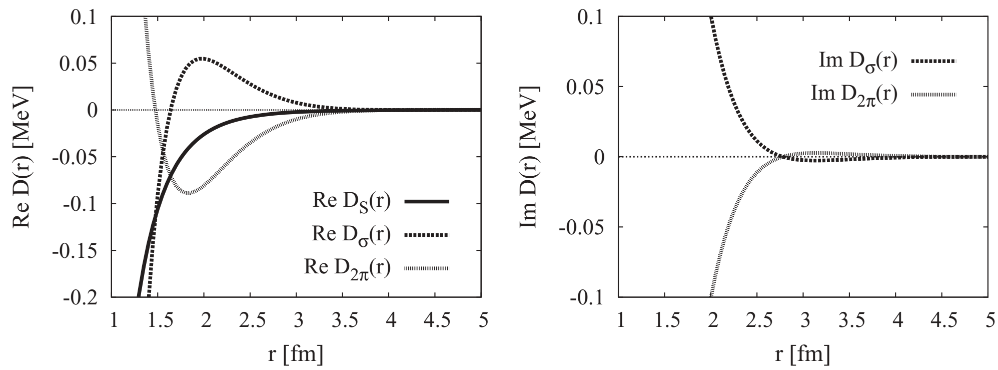

FIG. 8. Correlated $\pi\pi$ coordinate space propagator $D(r)$ (in MeV) as a function of the distance (in femtometers) for the $\pi\pi$ scattering toy model. In the left panel we draw the real part. We separate the pole contribution $D_\sigma(r)$ (dashed-dotted line) from the continuum contribution $D_{2\pi}(r)$ (dotted-line) and the total result $D(r)$ (solid line). The identity $D(r) = D_\sigma(r) + D_{2\pi}(r)$ is verified. In the right panel we show the cancellation of imaginary parts, $\mathrm{Im}D_\sigma(r) = -\mathrm{Im}D_{2\pi}(r)$.

Despite the large σ width $m_\sigma \sim \gamma_\sigma$ this expansion works because of the $1/8$ factor (with the next correction having a numerical value of $1/128$; see the following). If we assume that the scattering amplitude is proportional to this propagator the corresponding $\pi\pi$ phase shift is then given by

$$e^{2i\delta_{00}(s)} = \frac{s - m_\sigma^2 - i m_\sigma \gamma_\sigma \sqrt{\frac{s-4m_\pi^2}{m_\sigma^2-4m_\pi^2}}}{s - m_\sigma^2 + i m_\sigma \gamma_\sigma \sqrt{\frac{s-4m_\pi^2}{m_\sigma^2-4m_\pi^2}}}. \tag{A5}$$

The parametrization is such that the standard Breit-Wigner definition of the resonance is fulfilled for the bare parameters,

$$\delta_{00}(m_\sigma^2) = \frac{\pi}{2}, \quad \gamma_\sigma = \frac{1}{m_\sigma \delta'_{00}(m_\sigma^2)}. \tag{A6}$$

Of course, in the limit of narrow resonances the two definitions are indistinguishable and we have $M_\sigma \to m_\sigma$ and $\Gamma_\sigma \to \gamma_\sigma$. If we use the pole position in the second Riemann sheet of the S matrix or equivalently the zero in the first Riemann sheet from Ref. [36], yielding the value $M_\sigma - i\Gamma_\sigma/2 = 441^{+16}_{-8} - i272^{+9}_{-12}$ MeV, we get

$$m_\sigma = 567(10)\ \text{MeV}, \quad \gamma_\sigma/2 = 276(10)\ \text{MeV}. \tag{A7}$$

From the small-width expansion, Eq. (A4), we get $m_\sigma = 554(10)$ MeV, despite the apparent large width. From Ref. [103] one has the magnitude of the residue $|R_\sigma| = 0.218^{+0.023}_{-0.012}\ \text{GeV}^2$ whereas we get $|R_\sigma| = 0.430\ \text{GeV}^2$. Note the 120(20)-MeV shift between the Breit-Wigner and the pole position. With these parameters the scattering length is $a_{00}m_\pi = 0.36$, which is clearly off the value $a_{00}m_\pi = 0.220(2)$ deduced from ChPT. The propagator satisfies the unsubtracted dispersion in Eq. (59), where the spectral function is given by

$$\rho(\mu^2) = \frac{1}{\pi} \frac{\gamma_\sigma m_\sigma \sqrt{m_\sigma^2 - 4m_\pi^2}\sqrt{\mu^2 - 4m_\pi^2}}{(m_\sigma^2 - 4m_\pi^2)(\mu^2 - m_\sigma^2)^2 + \gamma_\sigma^2 m_\sigma^2 (\mu^2 - 4m_\pi^2)}, \tag{A8}$$

and satisfies the normalization condition given by Eq. (62) with $Z_\sigma = 1$. Thus, using the Fourier transformation of the propagator and separating explicitly the contribution from the poles $D_\sigma(r)$ and the 2π background $D_{2\pi}(r)$ we reproduce Eq. (65). This yields the result depicted in Fig. 8, which illustrates and checks the pole-background decomposition and shows that the *total* contribution, although describable by a Yukawa shape, *does not* correspond to the pole piece. In addition the cancellation of imaginary parts, $\mathrm{Im}D_\sigma(r) = -\mathrm{Im}D_{2\pi}(r)$, is explicitly verified. By using the inverse relations of Eq. (A4), in the narrow-width approximation the pole contribution becomes

$$\mathrm{Re}D_\sigma(r) = -\frac{e^{-M_\sigma r}}{4\pi r} \times \left[1 + \frac{r\Gamma_\sigma^2}{8}\left(\frac{2M_\sigma}{M_\sigma^2 - 4m_\pi^2} - r\right) + \cdots\right], \tag{A9}$$

in qualitative agreement with Eq. (67). However, the 2π contribution at long distances becomes

$$\begin{aligned} D_{2\pi}(r) &= -\frac{K_2(2m_\pi r)}{r^2} \frac{\gamma_\sigma m_\pi^2 m_\sigma}{\pi^2 (m_\sigma^2 - 4m_\pi^2)^{\frac{5}{2}}} + \cdots \\ &= -\frac{e^{-2m_\pi r}}{r^{\frac{5}{2}}} \frac{\gamma_\sigma m_\pi^{\frac{3}{2}} m_\sigma}{\pi^{\frac{3}{2}} (m_\sigma^2 - 4m_\pi^2)^{\frac{5}{2}}} + \cdots. \end{aligned} \tag{A10}$$

The asymptotic form in the first lime reproduces with 95% accuracy the full result, Eq. (65), for $r > 5$ fm. Finally, the ρ meson propagator and the associated $(I, J) = (1, 1)$ phase shift can be dealt with *mutatis mutandis* by using

$$[D_V(s)]^{-1} = s - m_\rho^2 - i m_\rho \gamma_\rho \left[\frac{s - 4m_\pi^2}{m_\rho^2 - 4m_\pi^2}\right]^{\frac{3}{2}}, \tag{A11}$$

where the p-wave character of the $\rho \to 2\pi$ decay can be recognized in the phase space factor.

APPENDIX B: REALISTIC SCALAR-ISOSCALAR $\pi\pi$ SCATTERING

Realistic parametrizations of the $\pi\pi$ scattering data have been proposed based on the conformal mappings [87,88] with several variations. Our results show little dependence on those and we show here the ghost-full version and the Adler zero located at the lowest order ChPT $s_A = m^2/2$ [87], which reads

$$\rho_{\pi\pi} \cot \delta_{00} = \frac{m^2}{s - m^2/2} \left[\frac{m}{\sqrt{s}} + B_0 + B_1 w + B_2 w^2 \right], \quad \text{(B1)}$$

with $w(s) = (\sqrt{s} - \sqrt{4m_K^2 - s})/(\sqrt{s} + \sqrt{4m_K^2 - s})$. For the three sets of $B_{0,1,2}$ parameters discussed in Ref. [87] the resulting complex pole position is slightly higher than the Roy equation value $\sqrt{s_\sigma} = 441^{+16}_{-8} - i272^{+9}_{-12}$ MeV [36]. If we use the dispersive representation for $D(r)$ given in Eq. (63) and cut the integral at the $\bar{K}K$ threshold $\mu = 2m_K$ we get a function that can be fitted in the range $1 \leqslant r \leqslant 5$ fm by a Yukawa potential with $m_\sigma = 600(50)$ MeV. The uncertainty corresponds to changing the $B_{0,1,2}$ parameters within errors [87] as well as varying the fitting interval. This is the modern version of the result found long ago [76] using a relativistic Breit-Wigner form (see Appendix A and Ref. [72]).

[1] E. Epelbaum, H.-W. Hammer, and U.-G. Meißner, Rev. Mod. Phys. (2008, in press), arXiv:0811.1338.
[2] R. Serber, *Serber Says: About Nuclear Physics* (World Scientific, Singapore, 1987).
[3] R. Serber, Annu. Rev. Nucl. Part. Sci. **44**, 1 (1994).
[4] J. Ashkin and T.-Y. Wu, Phys. Rev. **73**, 973 (1948).
[5] H. A. Bethe and P. Morrison, *Elementary Nuclear Theory* (Wiley, New York, 1956).
[6] R. S. Christian, Rep. Prog. Phys. **15**, 68 (1952).
[7] J. Blatt and V. Weisskopf, *Theoretical Nuclear Physics* (Wiley, New York, 1952).
[8] R. S. Christian and E. W. Hart, Phys. Rev. **77**, 441 (1950).
[9] E. Gerjuoy, Phys. Rev. **77**, 568 (1950).
[10] K. Nakabayasi and I. Sato, Phys. Rev. **88**, 144 (1952).
[11] R. Jastrow, Phys. Rev. **81**, 165 (1951).
[12] M. H. Hull, K. E. Lassila, H. M. Ruppel, F. A. McDonald, and G. Breit, Phys. Rev. **122**, 1606 (1961).
[13] M. F. de la Ripelle, S. A. Sofianos, and R. M. Adam, Ann. Phys. **316**, 107 (2005).
[14] A. Fetter and J. Walecka, *Quantum Theory of Many-Panicle Systems* (McGraw Hill, New York, 1971).
[15] H. A. Bethe and C. Longmire, Phys. Rev. **77**, 647 (1950).
[16] Y. A. Lashko and G. F. Filippov, Phys. At. Nucl. **70**, 1440 (2007).
[17] S. Ali, A. A. Z. Ahmad, and N. Ferdous, Rev. Mod. Phys. **57**, 923 (1985).
[18] T. Skyrme, Nucl. Phys. **9**, 615 (1959).
[19] E. Chabanat, J. Meyer, P. Bonche, R. Schaeffer, and P. Haensel, Nucl. Phys. **A627**, 710 (1997).
[20] M. Zalewski, J. Dobaczewski, W. Satula, and T. R. Werner, Phys. Rev. C **77**, 024316 (2008).
[21] V. G. J. Stoks, R. A. M. Klomp, M. C. M. Rentmeester, and J. J. de Swart, Phys. Rev. C **48**, 792 (1993).
[22] V. G. J. Stoks, R. A. M. Klomp, C. P. F. Terheggen, and J. J. de Swart, Phys. Rev. C **49**, 2950 (1994).
[23] N. Ishii, S. Aoki, and T. Hatsuda, Phys. Rev. Lett. **99**, 022001 (2007).
[24] S. R. Beane, P. F. Bedaque, K. Orginos, and M. J. Savage, Phys. Rev. Lett. **97**, 012001 (2006).
[25] A. Calle Cordon and E. Ruiz Arriola, Phys. Rev. C **78**, 054002 (2008).
[26] E. Wigner, Phys. Rev. **51**, 106 (1937).
[27] F. Hund, Z. Phys. D **105**, 202 (1937).
[28] G. 't Hooft, Nucl. Phys. **B72**, 461 (1974).
[29] E. Witten, Nucl. Phys. **B160**, 57 (1979).
[30] A. V. Manohar, *Talk given at the Les Houches Summer School in Theoretical Physics, Session 68, Les Houches, France, 28 July–5 September 1997, Probing the standard model of particle interactions, Pt. 2*, edited by F. David and R. Gupta (Les Houches 1999), pp. 1091–1169.
[31] E. E. Jenkins, Annu. Rev. Nucl. Part. Sci. **48**, 81 (1998).
[32] R. F. Lebed, Czech. J. Phys. **49**, 1273 (1999).
[33] D. B. Kaplan and M. J. Savage, Phys. Lett. **B365**, 244 (1996).
[34] D. B. Kaplan and A. V. Manohar, Phys. Rev. C **56**, 76 (1997).
[35] M. K. Banerjee, T. D. Cohen, and B. A. Gelman, Phys. Rev. C **65**, 034011 (2002).
[36] I. Caprini, G. Colangelo, and H. Leutwyler, Phys. Rev. Lett. **96**, 132001 (2006).
[37] C. Amsler *et al.* (Particle Data Group), Phys. Lett. **B667**, 1 (2008).
[38] R. B. Wiringa, V. G. J. Stoks, and R. Schiavilla, Phys. Rev. C **51**, 38 (1995).
[39] S. K. Bogner, T. T. S. Kuo, and A. Schwenk, Phys. Rep. **386**, 1 (2003).
[40] J. D. Holt, T. T. S. Kuo, G. E. Brown, and S. K. Bogner, Nucl. Phys. **A733**, 153 (2004).
[41] D. R. Entem, E. Ruiz Arriola, M. Pavon Valderrama, and R. Machleidt, Phys. Rev. C **77**, 044006 (2008).
[42] N. Kaiser, S. Gerstendorfer, and W. Weise, Nucl. Phys. **A637**, 395 (1998).
[43] N. Kaiser, R. Brockmann, and W. Weise, Nucl. Phys. **A625**, 758 (1997).
[44] M. C. M. Rentmeester, R. G. E. Timmermans, J. L. Friar, and J. J. de Swart, Phys. Rev. Lett. **82**, 4992 (1999).
[45] D. R. Entem and R. Machleidt, Phys. Rev. C **68**, 041001(R) (2003).
[46] S. K. Bogner, R. J. Furnstahl, S. Ramanan, and A. Schwenk, Nucl. Phys. **A784**, 79 (2007).
[47] M. Pavon Valderrama and E. Ruiz Arriola (in preparation).
[48] R. Machleidt, K. Holinde, and C. Elster, Phys. Rep. **149**, 1 (1987).
[49] G. Ecker, J. Gasser, A. Pich, and E. de Rafael, Nucl. Phys. **B321**, 311 (1989).
[50] E. Epelbaum, U. G. Meissner, W. Gloeckle, and C. Elster, Phys. Rev. C **65**, 044001 (2002).
[51] E. Epelbaum, W. Gloeckle, and U.-G. Meissner, Eur. Phys. J. A **19**, 401 (2004).
[52] R. Machleidt, Phys. Rev. C **63**, 024001 (2001).
[53] A. V. Belitsky and T. D. Cohen, Phys. Rev. C **65**, 064008 (2002).
[54] T. D. Cohen, Phys. Rev. C **66**, 064003 (2002).
[55] T. D. Cohen and B. A. Gelman, Phys. Lett. **B540**, 227 (2002).
[56] T. D. Cohen and D. C. Dakin, Phys. Rev. C **68**, 017001 (2003).
[57] E. Ruiz Arriola and A. Calle Cordon, Talk given at International Workshop on Effective Field Theories: From the Pion to the Upsilon (EFT 09) Valencia, Spain, 2–6 February 2009, PoS (EFT 09), 046 (2009).
[58] E. L. Lomon, Phys. Rev. D **26**, 576 (1982).
[59] M. J. Savage, Phys. Rev. C **55**, 2185 (1997).

[60] M. Pavon Valderrama and E. Ruiz Arriola, Phys. Rev. C **74**, 054001 (2006).
[61] S. Weinberg, Phys. Rev. Lett. **65**, 1177 (1990).
[62] M. Svec, Phys. Rev. D **55**, 5727 (1997).
[63] E. Megias, E. Ruiz Arriola, L. L. Salcedo, and W. Broniowski, Phys. Rev. D **70**, 034031 (2004).
[64] J. A. Oller, E. Oset, and J. R. Pelaez, Phys. Rev. Lett. **80**, 3452 (1998).
[65] J. Nieves and E. Ruiz Arriola, Nucl. Phys. **A679**, 57 (2000).
[66] J. Nieves, M. Pavon Valderrama, and E. Ruiz Arriola, Phys. Rev. D **65**, 036002 (2002).
[67] M. H. Partovi and E. L. Lomon, Phys. Rev. D **2**, 1999 (1970).
[68] W. Lin and B. D. Serot, Nucl. Phys. **A512**, 637 (1990).
[69] H.-C. Kim, J. W. Durso, and K. Holinde, Phys. Rev. C **49**, 2355 (1994).
[70] E. Oset, H. Toki, M. Mizobe, and T. T. Takahashi, Prog. Theor. Phys. **103**, 351 (2000).
[71] M. M. Kaskulov and H. Clement, Phys. Rev. C **70**, 014002 (2004).
[72] J. F. Donoghue, Phys. Lett. **B643**, 165 (2006).
[73] V. G. J. Stoks and T. A. Rijken, Nucl. Phys. **A613**, 311 (1997).
[74] R. J. Furnstahl, B. D. Serot, and H.-B. Tang, Nucl. Phys. **A615**, 441 (1997).
[75] P. Papazoglou *et al.*, Phys. Rev. C **59**, 411 (1999).
[76] J. Binstock and R. Bryan, Phys. Rev. D **4**, 1341 (1971).
[77] T. E. O. Ericson and W. Weise, *Pions and Nuclei* (Clarendon, Oxford, 1988).
[78] M. H. Johnson and E. Teller, Phys. Rev. **98**, 783 (1955).
[79] N. A. Tornqvist and M. Roos, Phys. Rev. Lett. **76**, 1575 (1996).
[80] W. M. Yao *et al.* (Particle Data Group), J. Phys. G **33**, 1 (2006).
[81] E. van Beveren, F. Kleefeld, G. Rupp, and M. D. Scadron, Mod. Phys. Lett. A **17**, 1673 (2002).
[82] A. Calle Cordon and E. Ruiz Arriola, AIP Conf. Proc. **1030**, 334 (2008).
[83] J. R. Pelaez, Phys. Rev. Lett. **92**, 102001 (2004).
[84] J. R. Pelaez and G. Rios, Phys. Rev. Lett. **97**, 242002 (2006).
[85] J. Nieves and E. R. Arriola (2009), arXiv:0904.4344.
[86] V. V. Flambaum and E. V. Shuryak, Phys. Rev. C **76**, 065206 (2007).
[87] R. Garcia-Martin, J. R. Pelaez, and F. J. Yndurain, Phys. Rev. D **76**, 074034 (2007).
[88] I. Caprini, Phys. Rev. D **77**, 114019 (2008).
[89] S. Weinberg, Phys. Rev. **177**, 2604 (1969).
[90] S. Weinberg, *Chiral Dynamics: Theory and Experiment: Proceedings of the Workshop Held at MIT, Cambridge, MA, USA, 25–29 July 1994*, edited by Aron M. Bernstein and Barry R. Holstein, vol. 452 *(Lecture Notes in Physics, 1995)*, pp. 1–13.
[91] J. Nieves and E. Ruiz Arriola (2009), arXiv:0904.4590.
[92] S. D. Protopopescu *et al.*, Phys. Rev. D **7**, 1279 (1973).
[93] B. Hyams *et al.*, Nucl. Phys. **B64**, 134 (1973).
[94] P. Estabrooks and A. D. Martin, Nucl. Phys. **B79**, 301 (1974).
[95] V. Srinivasan *et al.*, Phys. Rev. D **12**, 681 (1975).
[96] R. Kaminski, L. Lesniak, and K. Rybicki, Z. Phys. C **74**, 79 (1997).
[97] W. Hoogland *et al.*, Nucl. Phys. **B126**, 109 (1977).
[98] C. D. Froggatt and J. L. Petersen, Nucl. Phys. **B129**, 89 (1977).
[99] A. C. Cordon and E. R. Arriola (2009), arXiv:0905.4933.
[100] M. Teper, PoS (LATTICE 2008), 022 (2008).
[101] G. S. Bali and F. Bursa, J. High Energy Phys. 09 (2008) 110.
[102] L. Del Debbio, B. Lucini, A. Patella, and C. Pica, J. High Energy Phys. 03 (2008) 062.
[103] H. Leutwyler, AIP Conf. Proc. **1030**, 46 (2008).